Nonlinear Dyn (2012) 67:1913–1941
DOI 10.1007/s11071-011-0118-z

ORIGINAL PAPER

Chaos control and modified projective synchronization of unknown heavy symmetric chaotic gyroscope systems via Gaussian radial basis adaptive backstepping control

Faezeh Farivar · Mahdi Aliyari Shoorehdeli · Mohammad Ali Nekoui · Mohammad Teshnehlab

Received: 12 January 2011 / Accepted: 1 June 2011 / Published online: 8 July 2011

Abstract This paper proposes the chaos control and the modified projective synchronization methods for unknown heavy symmetric chaotic gyroscope systems via Gaussian radial basis adaptive backstepping control. Because of the nonlinear terms of the gyroscope system, the system exhibits chaotic motions. Occasionally, the extreme sensitivity to initial states in a system operating in chaotic mode can be very destructive to the system because of unpredictable behavior. In order to improve the performance of a dynamic system or avoid the chaotic phenomena, it is necessary to control a chaotic system with a regular or periodic motion beneficial for working with a particular condition. As chaotic signals are usually broadband and noise-like, synchronized chaotic systems can be used as cipher generators for secure communication. Obviously, the importance of obtaining these objectives is specified when the dynamics of gyroscope system are unknown. In this paper, using the neural backstepping control technique, control laws are established which guarantees the chaos control and the modified projective synchronization of unknown chaotic gyroscope system. In the neural backstepping control, Gaussian radial basis functions are utilized to on-line estimate the system dynamic functions. Also, the adaptation laws of the on-line estimators are derived in the sense of Lyapunov function. Thus, the unknown chaotic gyroscope system can be guaranteed to be asymptotically stable. Also, the control objectives have been achieved.

The proposed method allows us to arbitrarily adjust the desired scaling by controlling the slave system. It is not necessary to calculate the Lyapunov exponents and the eigenvalues of the Jacobian matrix, which makes it simple and convenient. Also, it is a systematic procedure for modified projective synchronization of chaotic systems and it can be applied to a variety of chaotic systems no matter whether it contains external excitation or not. Notice that it needs only one controller to realize modified projective synchronization no matter how much dimensions the chaotic system

F. Farivar (✉)
Department of Mechatronics Engineering, Science and Research Branch, Islamic Azad University, P.O. Box 14515/775, Tehran, Iran
e-mail: F.Farivar@srbiau.ac.ir

F. Farivar
e-mail: Faezeh_Farivar84@yahoo.com

M. Aliyari Shoorehdeli
Faculty of Electrical Engineering, Department of Mechatronics Engineering, K.N. Toosi University of Technology, Tehran, Iran
e-mail: Aliyari@eetd.kntu.ac.ir

M.A. Nekoui · M. Teshnehlab
Faculty of Electrical Engineering, Department of Control Engineering, K.N. Toosi University of Technology, Tehran, Iran

M.A. Nekoui
e-mail: Manekoui@eetd.kntu.ac.ir

M. Teshnehlab
e-mail: Teshnehlab@eetd.kntu.ac.ir

contains and the controller is easy to be implemented. It seems that the proposed method can be useful for practical applications of chaotic gyroscope systems in the future.

Numerical simulations are presented to verify the proposed control and synchronization methods.

Keywords Chaos control · Synchronization · Heavy symmetric gyroscope · Adaptive control · Backstepping control · Gaussian radial basis function neural network

1 Introduction

Dynamic chaos is a very interesting nonlinear effect which has been intensively studied during the last three decades. Chaotic phenomena can be found in many scientific and engineering fields such as biological systems, electronic circuits, power converters, chemical systems, and so on [1]. A chaotic system has complex dynamical behaviors that possess some special features, such as excessive sensitivity to initial conditions, broad spectrums of Fourier transform, bounded and fractal properties of the motion in the phase space, etc. Chaos in control systems and controlling chaos in dynamical systems have both attracted much interest in recent years. Since the pioneering work of Ott, Grebogi, and Yorke proposed the well-known OGY control method, where the control of chaotic systems has been widely studied [2]. Chaos control can be mainly divided into two categories [3]: one is the suppression of the chaotic dynamical behavior and the other is to generate or enhance chaos in nonlinear systems. Nowadays, different techniques have been proposed to achieve chaos control [4–6].

The synchronization problem is interpreted as a stabilization one. The goal is to stabilize, at the origin, the discrepancy between the master and slave systems. Discrepancy is defined as the dynamical differences between the master and slave systems and includes [7]:

1. Model mismatches, which means that the model of the master system might not be the same as that of the slave system.
2. Unknown initial conditions, which implies that the time series of the master system cannot be equal to that for the slave system.
3. Parametric uncertainty, which means that the slave system could be constructed with inaccuracies.

Since the synchronization of chaotic dynamical systems has been observed by Pecora and Carroll [8] in 1990, chaos synchronization has become a topic of great interest [9–11]. Synchronization phenomena have been reported in the recent literature. Until now, different types of synchronization have been found in interacting chaotic systems, such as complete synchronization [8], generalized synchronization [12], phase synchronization [13], and antiphase synchronization [14], etc.

In 1999, projective synchronization has been first reported by Mainieri and Rehacek [15] in partially linear systems that the master and slave vectors synchronize up to a constant scaling factor α (a proportional relation). Later, some researchers have extended synchronization to a general class of chaotic systems without the limitation of partial-linearity, such as nonpartially-linear systems [16, 17]. After that, a new synchronization, called generalized projective synchronization (GPS), has been observed in the nonlinear chaotic systems [18–20].

Recently, Li [21] considers a new synchronization method, called modified projective synchronization (MPS), where the responses of the synchronized dynamical states synchronize up to a constant scaling matrix. Therefore, the synchronization and anti-synchronization can coexist in a chaos synchronization problem.

The dynamics of a gyro is a very interesting nonlinear problem in classical mechanics. The concept of chaotic motion in a gyro was first presented in 1981 by Leipnik and Newton [22], showing the existence of two strange attractors. The gyro has attributes of great utility to navigational, aeronautical, and space engineering [23]. Gyros for sensing angular motion are used in airplane automatic pilots, rocket-vehicle launch-guidance, space-vehicle attitude systems, ship's gyrocompasses, and submarine inertial auto-navigators. In the past years, gyros have been found with rich phenomena which give benefit for the understanding of gyro systems. Different types of gyros with linear/nonlinear damping are investigated for predicting the dynamic responses such as periodic and chaotic motions [24–29].

Some methods have been presented to control of the nonlinear gyro system such as delayed feedback control and adaptive control [25], backstepping control [30], sliding mode control [31]. Also, some methods have been presented to synchronize two identi-

cal/nonidentical nonlinear gyro systems such as active control [32, 33], backstepping control [30, 34], adaptive sliding mode control [35], fuzzy control [36], fuzzy sliding mode control [37], neural sliding mode control [38, 39], and some methods so on [40–45].

In some studies, the chaotic gyroscope system is considered as a model with parametric uncertainty [35, 43], model uncertainty [36], and external disturbance plus model uncertainty [38–40]. No one is considered this system as an unknown system.

Numerous backstepping control design procedures have been proposed to achieve chaos control and synchronization [6, 20, 30, 34, 46]. The key idea of backstepping design is to select recursively some appropriate functions of state variables as virtual control inputs for lower dimension subsystems of the overall system [47].

Notice that for some chaotic systems, since the dynamic characteristics of the control system are nonlinear and the precise models are difficult to obtain, the model-based control approaches are difficult to be implemented [48].

The adaptive neural control approach based on backstepping design has been developed for nonlinear uncertain systems without the requirement of matching conditions. Stable neural controller design schemes are proposed for unknown nonlinear SISO systems via backstepping design technique [49–51]. With the backstepping design technique, neural networks are mostly applied to approximate the unmatched and unknown nonlinearities, and then implement adaptive control using the conventional control technology. The advantage of adaptive neural control based on backstepping methodology includes that both the parameters and the nonlinear functions can be unknown and the uncertainties in systems need not satisfy the matching conditions [52]. Excellent contributions for backstepping control, using neural networks, are presented in [53–67].

Overview of this study In spite of several notable studies of heavy symmetric chaotic gyroscope system, there has not been a rigorous treatment of chaos control and synchronization of unknown chaotic gyroscope system. This topic is an interesting topic in the framework of intelligent hybrid control theory. The discussion in this paper may be viewed as an attempt to intelligent nonlinear hybrid control and synchronization of unknown heavy symmetric gyroscope system as a "*mechatronical control system.*"

This paper proposes the chaos control and modified projective synchronization of unknown heavy symmetric chaotic gyroscope systems via Gaussian Radial Basis Adaptive Backstepping Control (GRBABC). The GRBABC system is composed of the Gaussian radial basis function neural networks ($GRBF_{NN}$) identification and adaptive backstepping control techniques. The control methods contain $GRBF_{NN}$ identifiers designed in the sense of the Lyapunov functions. The $GRBF_{NN}$ identifiers are utilized to online estimate the system dynamic functions. An adaptation laws for GRBABC system is derived in the sense of Lyapunov function. Thus, the system can be guaranteed to be asymptotically stable.

Contribution of this study For some systems, since the dynamic characteristics of the control system are nonlinear and the precise models are difficult to obtain, the model-based control approaches are difficult to be implemented. To overcome this drawback, a novel Gaussian radial basis adaptive backstepping control (GRBABC) system has been proposed. In the neural nonlinear controller, a $GRBF_{NN}$ identifier is utilized to estimate the system dynamic function in an online manner. The adaptive law of the GRBABC system is synthesized using the Lyapunov functions so that the asymptotic stability of the control system can be guaranteed.

Suppression of the chaos is presented so as to improve the performance of a dynamical system. Proposed methods in this study to achieve modified projective synchronization (MPS) are capable to create a full range GPS of all state variables in a proportional way, but the complete synchronization is not considered in the proposed method. It also allows us to arbitrarily adjust the desired scaling by controlling the slave system. It is not necessary to calculate the Lyapunov exponents and the eigenvalues of the Jacobian matrix, which makes it simple and convenient.

The proposed method is a systematic procedure for control and synchronization of uncertain chaotic systems. It can be applied to a variety of chaotic systems no matter whether it contains external excitation or not. It needs only one control system to realize chaos control and synchronization no matter how many dimensions the chaotic system contains. The controller is easy to be implemented.

Since the gyro has been utilized to describe the mode in navigational, aeronautical or space engineering, the chaos control and MPS procedure of chaotic

gyroscope systems in this study may have practical applications in the future.

This paper is organized as follows. In Sect. 2, the dynamics of a heavy symmetric gyroscope system has been explained. Chaos control problem and modified projective synchronization problem have been formulated in Sect. 3. In Sect. 4, the ideal backstepping controls have been designed to chaos control and modified projective synchronization of chaotic gyroscope systems. Also, two theorems for chaos control and MPS of gyroscopes via ideal backstepping control have been proven in Sect. 4. Then it is assumed that the dynamic characteristics of the gyroscope system are unknown. It has been explained in Sect. 5. Also, in this section, GRBF_{NN} identifier is described. GRBABC system is designed to chaos control and MPS of chaotic gyroscope systems in Sects. 6 and 7, respectively. Moreover, two theorems for chaos control and MPS of gyroscopes via GRBABC have been proven in Sects. 6 and 7, respectively. In Sect. 8, novelty of proposed method has been explained. Finally, to show the effectiveness of the proposed control methods for chaos control and synchronization of gyroscope systems, simulations have been presented in Sect. 9. At the end, the paper is concluded in Sect. 10.

2 Description of chaotic gyroscope system

The symmetric gyroscope mounted on a vibrating base is shown in Fig. 1. The dynamics of a heavy symmetric gyroscope with linear-plus-cubic damping of angle θ mounted on a vibrating base can be described by Euler's angels θ, ϕ and ψ. The vibration dynamics of the base can be described by the multiple harmonic motion $\sum_{k=1}^{n} A_k \sin \omega_k t \sin x$.

Let the state variables $x = [\theta\ \dot{\theta}\ \dot{\phi}]^T$, then the dynamic equations can be obtained as (more details are presented in Appendix A):

$$\begin{cases} \dot{x}_1 = x_2 \\ \dot{x}_2 = -\dfrac{(\beta_\phi - \beta_\psi \cos x_1)(B_\psi - \beta_\phi \cos x_1)}{I_1^2 \sin^3 x_1} \\ \qquad\quad - \dfrac{c_1}{I_1} x_2 + \dfrac{M_g l}{I_1} \sin x_1 - \dfrac{M_g A}{I_1} \sin \omega t \sin x_1 \\ \dot{x}_3 = -2 x_2 x_3 \dfrac{\cos x_1}{\sin x_1} + \dfrac{\beta_\psi}{I_1 \sin x_1} x_2 \end{cases} \tag{1}$$

where I_1 and I_3 are the polar and equatorial moments of inertia of the typical gyroscope, M_g is the gravity force, l is the distance between the center of gravity and O.

It is clear that coordinates θ and ϕ are cyclic, which provides the conjugate momenta. The momentum integrals are β_ϕ and β_ψ.

The gyroscope system (1) performs complex dynamics and has been extensively studied Ge [24].

With specific value set as follows:

$$\beta_\phi = 2, \quad \beta_\psi = 5, \quad l = 0.25, \quad I_1 = 1$$
$$M_g = 4, \quad c_1 = 0.5, \quad \omega = 2, \quad A = 50$$

In numeric simulation, the dynamic behavior gyroscope system (2) exhibits an irregular motion as shown in Figs. 2 and 3 with initial conditions of

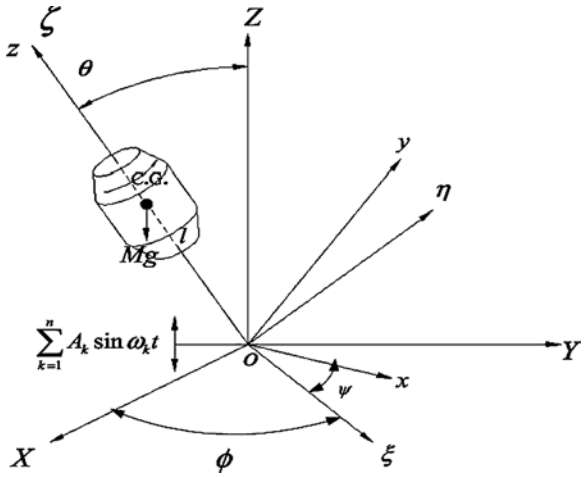

Fig. 1 A schematic diagram of a heavy symmetric gyroscope

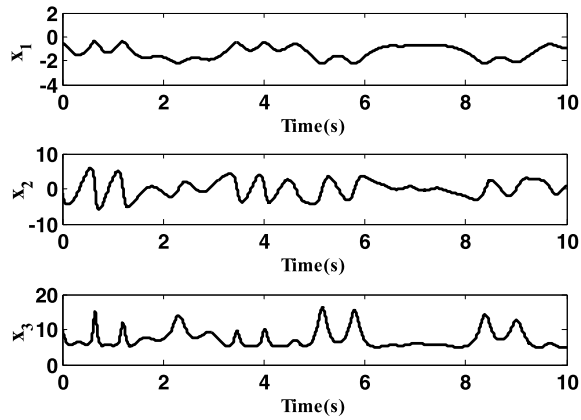

Fig. 2 Time series of x_1, x_2, and x_3

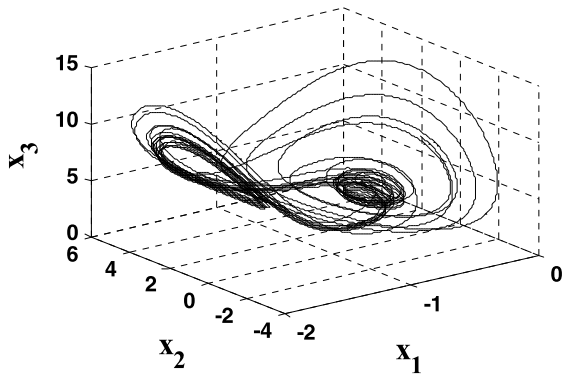

Fig. 3 Phase plane trajectory of a chaotic nonlinear gyro

$$(x_1, x_2, x_3) = (-0.5, -1.2, 10)$$

Figures 2 and 3 show that the gyroscope system trajectories are in a state of chaotic motion.

Following this, the chaos control problem of nonlinear chaotic gyros is described.

3 Chaos control and modified synchronization problems of chaotic gyroscope system

In this section, the chaos control problem and modified projective synchronization problem have been formulated as follows.

3.1 Chaos control problem of chaotic gyroscope system

In the previous section, it has been shown that the heavy symmetric gyro considered exhibits chaotic motion. The extreme sensitivity to initial states in a system operating in chaotic mode can be very destructive to the system because of unpredictable behavior. Sometimes, chaos is unwanted or undesirable. In order to improve the performance of a dynamic system or avoid the chaotic phenomena, we need to control a chaotic system with a periodic motion which is beneficial for working with a particular condition. It is thus of great practical importance to develop suitable control methods. Many researchers have been focused on this type of problem controlling chaos. Anticontrol of chaos is interesting, nontraditional, and very challenging.

For this purpose, in this section, chaos control problem of gyroscope system is described as follows.

Now, control inputs are introduced in (1) for the second and third states. Thus, the controlled nonlinear gyro becomes as follows:

$$\begin{cases} \dot{x}_1 = x_2 \\ \dot{x}_2 = -\dfrac{(\beta_\phi - \beta_\psi \cos x_1)(B_\psi - \beta_\phi \cos x_1)}{I_1^2 \sin^3 x_1} \\ \qquad\quad - \dfrac{c_1}{I_1} x_2 + \dfrac{M_g l}{I_1} \sin x_1 \\ \qquad\quad - \dfrac{M_g A}{I_1} \sin \omega t \sin x_1 + u_1(t) \\ \dot{x}_3 = -2x_2 x_3 \dfrac{\cos x_1}{\sin x_1} + \dfrac{\beta_\psi}{I_1 \sin x_1} x_2 + u_2(t) \end{cases} \tag{2}$$

where $u_1, u_2 \in R$ are the control inputs attached in the nonlinear gyroscope system.

In order to simplify the following procedure, two nonlinear functions are defined as follows:

$$\begin{cases} g(x_1, x_2) = -\dfrac{(\beta_\phi - \beta_\psi \cos x_1)(B_\psi - \beta_\phi \cos x_1)}{I_1^2 \sin^3 x_1} \\ \qquad\quad - \dfrac{c_1}{I_1} x_2 + \dfrac{M_g l}{I_1} \sin x_1 \\ \qquad\quad - \dfrac{M_g A}{I_1} \sin \omega t \sin x_1 \\ h(x_1, x_2, x_3) = -2x_2 x_3 \dfrac{\cos x_1}{\sin x_1} + \dfrac{\beta_\psi}{I_1 \sin x_1} x_2 \end{cases} \tag{3}$$

The control problem is to drive the system to track a three-dimensional desired vector $X_d(t)$ as follows:

$$\begin{aligned} X_d(t) &= [x_{d\_1}, x_{d\_2}, x_{d\_3}]^T \\ &= [x_{d\_1}, \dot{x}_{d\_1}, x_{d\_2}]^T \end{aligned} \tag{4}$$

which belongs to a class of C function on $[t_0, \infty)$. Let us define the tracking error as

$$\begin{aligned} E(t) &= \left[e_1(t), e_2(t), e_3(t)\right]^T \\ &= [x_1 - x_{d\_1}, x_2 - \dot{x}_{d\_1}, x_3 - x_{d\_3}]^T \end{aligned} \tag{5}$$

Then the error dynamics can be obtained from (5), (2), and (3) as follows:

$$\begin{cases} \dot{e}_1 = e_2 \\ \dot{e}_2 = g(x_1, x_2) - \ddot{x}_{d\_1} + u_1(t) \\ \dot{e}_3 = h(x_1, x_2, x_3) - \dot{x}_{d\_3} + u_2(t) \end{cases} \tag{6}$$

The control goal considered in this section is that for any given target orbit $X_d(t)$, the controller is designed such that the resulting tracking error vector satisfies:

$$\lim_{t\to\infty} \|E(t)\| \to 0 \tag{7}$$

where $\|\cdot\|$ is the Euclidean norm of a vector.

3.2 Chaos synchronization problem of chaotic gyroscope systems

Consider two coupled, chaotic gyro systems, where the master and slave systems are denoted by x and y, respectively. The master system is shown in (1) and the slave system is presented as follows:

$$\begin{cases} \dot{y}_1 = y_2 \\ \dot{y}_2 = -\dfrac{(\beta_\phi - \beta_\psi \cos y_1)(B_\psi - \beta_\phi \cos y_1)}{I_1^2 \sin^3 y_1} \\ \qquad - \dfrac{c_1}{I_1} y_2 + \dfrac{M_g l}{I_1} \sin y_1 \\ \qquad - \dfrac{M_g A}{I_1} \sin \omega t \sin y_1 + u_1(t) \\ \dot{y}_3 = -2 y_2 y_3 \dfrac{\cos y_1}{\sin y_1} + \dfrac{\beta_\psi}{I_1 \sin y_1} y_2 + u_2(t) \end{cases} \tag{8}$$

In order to simplify the following procedure, two nonlinear functions are defined as follows:

$$\begin{cases} g(y_1, y_2) = -\dfrac{(\beta_\phi - \beta_\psi \cos y_1)(B_\psi - \beta_\phi \cos y_1)}{I_1^2 \sin^3 y_1} \\ \qquad - \dfrac{c_1}{I_1} y_2 + \dfrac{M_g l}{I_1} \sin y_1 \\ \qquad - \dfrac{M_g A}{I_1} \sin \omega t \sin y_1 \\ h(y_1, y_2, y_3) = -2 y_2 y_3 \dfrac{\cos y_1}{\sin y_1} + \dfrac{\beta_\psi}{I_1 \sin y_1} y_2 \end{cases} \tag{9}$$

Defining the generalized synchronization errors between the master and slave systems as follows:

$$E(t) = \begin{bmatrix} e_1 \\ e_2 \\ e_3 \end{bmatrix} = \begin{bmatrix} y_1 \\ y_2 \\ y_3 \end{bmatrix} - \begin{bmatrix} \alpha_1 & 0 & 0 \\ 0 & \alpha_1 & 0 \\ 0 & 0 & \alpha_2 \end{bmatrix} \begin{bmatrix} x_1 \\ x_2 \\ x_3 \end{bmatrix} \tag{10}$$

where $\alpha_1, \alpha_2 \in R$ are the scaling factors that define a proportional relation between the synchronized systems. Obviously, the modified projective synchronization is defined as the generalized projective synchronization if α_1 is equal to α_2. Moreover, it is considered that $\alpha_1, \alpha_2 \neq 1$. Then the error dynamics can be obtained as

$$\begin{cases} \dot{e}_1(t) = e_2(t) \\ \dot{e}_2(t) = g(y_1, y_2) - \alpha_1 g(x_1, x_2) + u_1(t) \\ \dot{e}_3(t) = h(y_1, y_2, y_3) - \alpha_2 h(x_1, x_2, x_3) + u_2(t) \end{cases} \tag{11}$$

Notice that in this study the MPS has been considered, then $\alpha \neq 1$:

$$\begin{cases} \dot{e}_1(t) = e_2(t) \\ \dot{e}_2(t) = (1 - \alpha_1) p(x_1, x_2, y_1, y_2, \alpha_1) + u_1(t) \\ \dot{e}_3(t) = (1 - \alpha_2) q(x_1, x_2, x_3, y_1, y_2, y_3, \alpha_2) + u_2(t) \end{cases} \tag{12}$$

where

$$\begin{cases} p(x_1, x_2, y_1, y_2, \alpha_1) = \dfrac{g(y_1, y_2) - \alpha_1 g(x_1, x_2)}{1 - \alpha_1} \\ q(x_1, x_2, x_3, y_1, y_2, y_3, \alpha_2) \\ \quad = \dfrac{h(y_1, y_2, y_3) - \alpha_2 h(x_1, x_2, x_3)}{1 - \alpha_2} \end{cases} \tag{13}$$

Notice that $\alpha_1, \alpha_2 \in R$ and $\alpha_1, \alpha_2 \neq 1$.

The objective of the current synchronization problem is to design the appropriate control signals $u_1(t)$ and $u_2(t)$ such that for any initial conditions of the master and slave systems, the synchronization errors converge to zero such that the resulting synchronization error vector satisfies (7).

In the next section, the backstepping control is designed to achieve the control and synchronization objectives.

4 Ideal backstepping control technique to chaos control and modified synchronization of chaotic gyroscopes

In this section, ideal backstepping control to chaos control and MPS have been designed as follows.

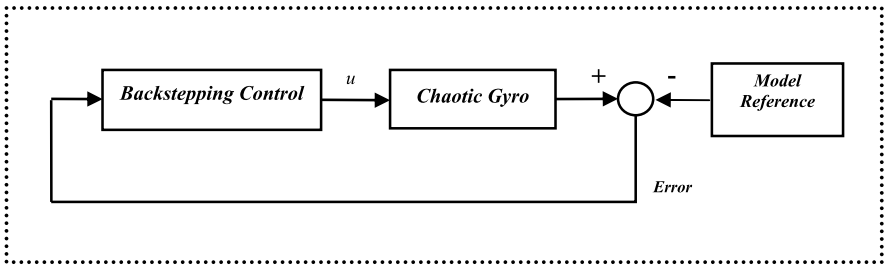

Fig. 4 Chaos control via backstepping control

4.1 Chaos control via backstepping control

The architecture of chaos control of gyroscope system via backstepping control is shown in Fig. 4. The following theorem shows the properties of chaos control of two-degree-of-freedom heavy symmetric gyroscope systems via backstepping control.

Theorem 1 *Consider the chaos control problem represented by* (6). *If the control inputs* $u_1(t)$ *and* $u_2(t)$ *are suitably designed as*:

$$u_1(t) = -k_1 e_2 - k_2 e_1 - g(x_1, x_2) + \ddot{x}_{d\_1} \tag{14}$$

$$u_2(t) = -k_3 e_3 - h(x_1, x_2, x_3) + \dot{x}_{d\_3} \tag{15}$$

where $k_1 = c_1 + c_2$, $k_2 = c_1 c_2$, $k_3 = c_3$, *and* c_i $(i = 1, 2, 3)$ *are positive constant parameters. Then the hitting condition of Lyapunov stability theory is satisfied, and the trajectories of chaos control error dynamics will converge to zero.*

Proof of Theorem 1 To obtain the control laws of (6), the design of ideal backstepping controller for chaos control is described step-by-step as follows:

Step 1 Define

$$z_1 = e_1 \tag{16}$$

and the derivative of e_1 is defined as

$$\dot{z}_1 = \varphi_1 \tag{17}$$

The φ_1 can be viewed as a virtual control in the equation.
Define a Lyapunov function as

$$V_1 = \frac{1}{2} z_1^2 \tag{18}$$

Differentiating (18) with respect to time and using (17), it is obtained that

$$\dot{V}_1 = z_1 \dot{z}_1 = z_1 \varphi_1 \tag{19}$$

Let

$$\varphi_1 = -c_1 z_1 \tag{20}$$

then

$$\dot{V}_1 = -c_1 z_1^2 \tag{21}$$

where c_1 is a positive constant parameter.
Step 2 Define

$$z_2 = e_2 - \varphi_1 \tag{22}$$

and the derivative of (22) is defined as

$$\dot{z}_2 = \dot{e}_2 - \dot{\varphi}_1 = g(x_1, x_2) - \ddot{x}_{d\_1} + u_1(t) - \dot{\varphi}_1 \tag{23}$$

Define a Lyapunov function as

$$V_2 = \frac{1}{2} z_2^2 \tag{24}$$

Differentiating (24) with respect to time and using (23), it is obtained that

$$\dot{V}_2 = z_2 \dot{z}_2 = z_2 \left(g(x_1, x_2) - \ddot{x}_{d\_1} + u_1(t) - \dot{\varphi}_1 \right) \tag{25}$$

Let

$$u_1(t) = -c_2 z_2 - g(x_1, x_2) + \ddot{x}_{d\_1} + \dot{\varphi}_1 \tag{26}$$

then

$$\dot{V}_2 = -c_2 z_2^2 \tag{27}$$

where c_2 is a positive constant parameter.

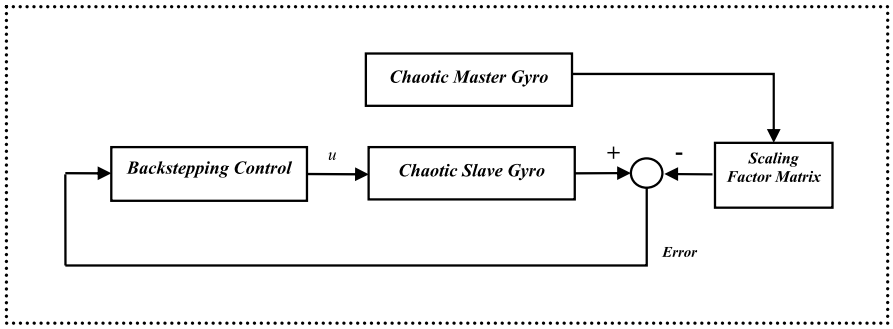

Fig. 5 MPS via backstepping control

Step 3 Define

$$z_3 = e_3 \tag{28}$$

and the derivative of e_3 is defined as

$$\dot{z}_3 = h(x_1, x_2, x_3) - \dot{x}_{d\_3} + u_2(t) \tag{29}$$

Define a Lyapunov function as

$$V_3 = \frac{1}{2} z_3^2 \tag{30}$$

Differentiating (30) with respect to time and using (29), it is obtained that

$$\dot{V}_3 = z_3 \dot{z}_3 = z_3 \big(h(x_1, x_2, x_3) - \dot{x}_{d\_3} + u_2(t)\big) \tag{31}$$

Let

$$u_2(t) = -c_3 z_3 - h(x_1, x_2, x_3) + \dot{x}_{d\_3} \tag{32}$$

then

$$\dot{V}_3 = -c_3 z_3^2 \tag{33}$$

where c_3 is a positive constant parameter.

Therefore, define the Lyapunov function as

$$V_T = V_1 + V_2 + V_3 \tag{34}$$

Differentiating (34) with respect to time and using (21), (27), and (33), we obtain

$$\dot{V}_T = -\sum_{i=1}^{3} c_i z_i^2 \tag{35}$$

where c_i $(i = 1, 2, 3)$ are positive constant parameters.

Then the backstepping controller for chaos control proposed in Theorem 1 will asymptotically stabilize the error dynamics. (Converging errors to zero are investigated in Appendix B.) □

4.2 Chaos synchronization via backstepping control

The architecture of MPS via backstepping control is shown in Fig. 5. The following theorem shows the properties of the MPS of two-degree-of-freedom gyroscope systems via backstepping control.

Theorem 2 *Consider the MPS problem represented by* (12). *If the control inputs* $u_1(t)$ *and* $u_2(t)$ *are suitably designed as*:

$$u_1(t) = -k_1 e_2 - k_2 e_1 - (1 - \alpha_1) p(x_1, x_2, y_1, y_2, \alpha_1) \tag{36}$$

$$u_2(t) = -k_3 e_3 - (1 - \alpha_2) q(x_1, x_2, x_3, y_1, y_2, y_3, \alpha_2) \tag{37}$$

where $k_1 = c_1 + c_2$, $k_2 = c_1 c_2$, $k_3 = c_3$, *and* c_i $(i = 1, 2, 3)$ *are positive constant parameters. Then the hitting condition of Lyapunov stability theory is satisfied, and the trajectories of chaos control error dynamics will converge to zero.*

Proof of Theorem 2 To obtain the control laws of (12), the design of ideal backstepping controller for MPS is described step-by-step as follows:

Step 1 Define

$$z_1 = e_1 \tag{38}$$

and the derivative of e_1 is defined as

$$\dot{z}_1 = \varphi_1 \tag{39}$$

The φ_1 can be viewed as a virtual control in the equation.

Define a Lyapunov function as

$$V_1 = \frac{1}{2} z_1^2 \tag{40}$$

Differentiating (40) with respect to time and using (39), it is obtained that

$$\dot{V}_1 = z_1 \dot{z}_1 = z_1 \varphi_1 \tag{41}$$

Let

$$\varphi_1 = -c_1 z_1 \tag{42}$$

then

$$\dot{V}_1 = -c_1 z_1^2 \tag{43}$$

where c_1 is a positive constant parameter.

Step 2 Define

$$z_2 = e_2 - \varphi_1 \tag{44}$$

and the derivative of (44) is defined as

$$\begin{aligned} \dot{z}_2 &= \dot{e}_2 - \dot{\varphi}_1 \\ &= (1-\alpha_1) p(x_1, x_2, y_1, y_2, \alpha_1) + u_1(t) - \dot{\varphi}_1 \end{aligned} \tag{45}$$

Define a Lyapunov function as

$$V_2 = \frac{1}{2} z_2^2 \tag{46}$$

Differentiating (46) with respect to time and using (45), it is obtained that

$$\begin{aligned} \dot{V}_2 &= z_2 \dot{z}_2 \\ &= z_2 \big[(1-\alpha_1) p(x_1, x_2, y_1, y_2, \alpha_1) + u_1(t) - \dot{\varphi}_1 \big] \end{aligned} \tag{47}$$

Let

$$u_1(t) = -c_2 z_2 - (1-\alpha_1) p(x_1, x_2, y_1, y_2, \alpha_1) + \dot{\varphi}_1 \tag{48}$$

then

$$\dot{V}_2 = -c_2 z_2^2 \tag{49}$$

where c_2 is a positive constant parameter.

Step 3 Define

$$z_3 = e_3 \tag{50}$$

and the derivative of e_3 is defined as

$$\dot{z}_3 = (1-\alpha_2) q(x_1, x_2, x_3, y_1, y_2, y_3, \alpha_2) + u_2(t) \tag{51}$$

Define a Lyapunov function as

$$V_3 = \frac{1}{2} z_3^2 \tag{52}$$

Differentiating (52) with respect to time and using (51), it is obtained that

$$\begin{aligned} \dot{V}_3 &= z_3 \dot{z}_3 \\ &= z_3 \big[(1-\alpha_2) q(x_1, x_2, x_3, y_1, y_2, y_3, \alpha_2) + u_2(t) \big] \end{aligned} \tag{53}$$

Let

$$u_2(t) = -c_3 z_3 - (1-\alpha_2) q(x_1, x_2, x_3, y_1, y_2, y_3, \alpha_2) \tag{54}$$

then

$$\dot{V}_3 = -c_3 z_3^2 \tag{55}$$

where c_3 is a positive constant parameter.

Therefore, define the Lyapunov function as

$$V_T = V_1 + V_2 + V_3 \tag{56}$$

Differentiating (56) with respect to time and using (43), (49), and (55), we obtain

$$\dot{V}_T = -\sum_{i=1}^{3} c_i z_i^2 \tag{57}$$

where c_i $(i = 1, 2, 3)$ are positive constant parameters.

Then the backstepping controller for MPS proposed in Theorem 2 will asymptotically stabilize the error dynamics. □

5 Design of GRBABC systems

Since the system dynamic functions of chaotic heavy symmetric gyroscope systems may be unknown or perturbed in practical application, the ideal backstepping controllers designed in Theorems 1 and 2 cannot be precisely obtained. To solve this problem, a GRBF_{NN} identifier is utilized to approximate the system dynamic function. The descriptions of the GRBF_{NN} identifier is described in this section. GRBABC system is designed to chaos control and MPS of chaotic gyroscope systems, in Sect. 6. Moreover, novelty of the proposed method is explained in Sect. 7.

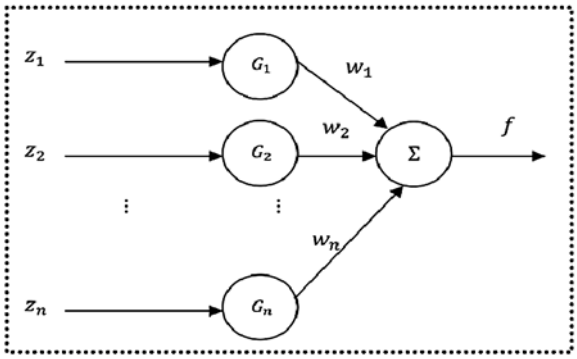

Fig. 6 Structure of GRBF neural network

5.1 GRBF_{NN} identifier

The network structure of the GRBF_{NN} identifier is shown in Fig. 6, which can be considered as one layer feed forward neural network with nonlinear element. The GRBF_{NN} output can perform the mapping according to

$$f(z) = \sum_{j=1}^{n} w_j G_j(z_j, m_j, \sigma_j) \tag{58}$$

where $z = [z_1, z_2, \ldots, z_n]^T \in R^n$ is the input vector, $G_j(z_j, m_j, \sigma_j) \in R^n$, $j = 1, 2, \ldots, n$ are the Gaussian radial basis function, $\sigma_j \in R$ is the spread of Gaussian function, m_j is the mean value of Gaussian function and n is the number of neurons. Each Gaussian radial basis function can be represented by

$$G_j(z_j, m_j, \sigma_j) = \exp\left(\frac{z_j - m_j}{\sqrt{2}\sigma_j}\right)^2 \tag{59}$$

Equation (58) can be rewritten in compact vector forms as

$$f(z, w, m, \sigma) = w^T G(z, m, \sigma) \tag{60}$$

where $w = [w_1, w_2, \ldots, w_n]^T$, $G = [G_1, G_2, \ldots, G_n]^T$, $m = [m_1, m_2, \ldots, m_n]^T$, $\sigma = [\sigma_1, \sigma_2, \ldots, \sigma_n]^T$.

By the universal approximation theorem, there exists an ideal GRBF_{NN} identifier f^* such that

$$f = f^*(z) + \Delta = w^{*T} G\left(z, m^*, \sigma^*\right) \tag{61}$$

where Δ denotes the approximation error and is assumed to be bounded. w^*, m^*, and σ^* are the optimal parameter vectors of w, m, and σ, respectively. The optimal parameter vectors that are needed to best approximate a given nonlinear function are difficult to determine. So, an estimate function is defined as

$$\hat{f}(z, \hat{w}, \hat{m}, \hat{\sigma}) = \hat{w}^T G(z, \hat{m}, \hat{\sigma}) \tag{62}$$

where $\hat{w}, \hat{m}$, and $\hat{\sigma}$ are the estimated of w^*, m^*, and σ^*, respectively. For notational convenience, denote

$$G^* = G\left(z, m^*, \sigma^*\right) \tag{63}$$

and

$$\hat{G} = G(z, \hat{m}, \hat{\sigma}) \tag{64}$$

Define

$$\tilde{w} = w^* - \hat{w} \tag{65}$$

Notice that the optimal values are not unique. Also, in this study, m and σ are not trained.

6 GRBABC system to chaos control of unknown chaotic gyroscope system

The architecture of proposed method to chaos control via Gaussian Radial Basis Adaptive Backstepping Control (*GRBABC*) system is shown in Fig. 7. The control laws of the GRBABC systems are developed as follows.

The neural backstepping controllers are chosen as follows to chaos control of unknown chaotic gyroscope system considered in (6):

$$u_1(t) = -k_1 e_2 - k_2 e_1 - \hat{g}(x_1, x_2) + \ddot{x}_{d\_1} \tag{66}$$

$$u_2(t) = -k_3 e_3 - \hat{h}(x_1, x_2, x_3) + \dot{x}_{d\_3} \tag{67}$$

where two GRBF_{NN} identifiers $\hat{g}$ and $\hat{h}$ are designed to online estimate the system dynamic functions g and h, restrictively. Follow theorem shows the properties of the proposed GRBABC system to chaos control of unknown chaotic gyroscope system considered in (6).

Theorem 3 *Consider the chaos control problem represented by* (6). *g and h are the unknown functions. The ideal control system is designed as* (14), (15). *The neural backstepping controllers are designed as* (66), (67), *in which the adaptation laws of the* GRBF_{NN} *identifiers are achieved as*

$$\dot{\hat{w}}_g = -\dot{\tilde{w}}_g = z_2 G_g \tag{68}$$

$$\dot{\hat{w}}_h = -\dot{\tilde{w}}_h = z_3 G_h \tag{69}$$

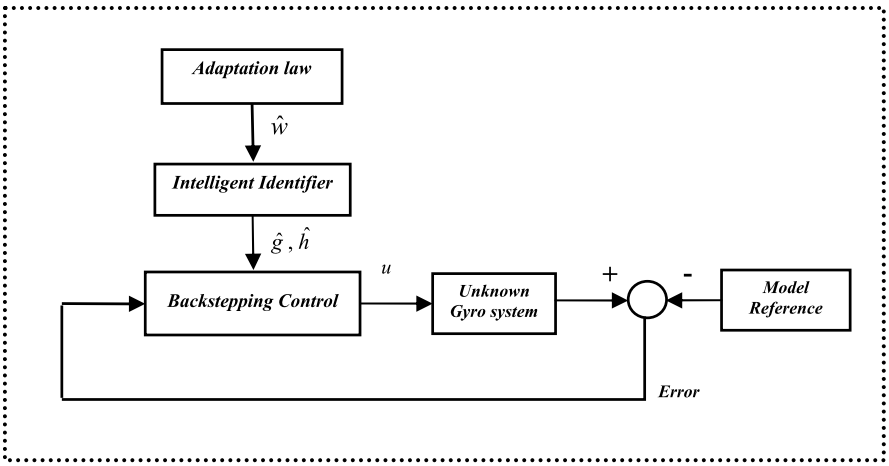

Fig. 7 Chaos Control via GRBABC system

where z_2 and z_3 are represented in (16) and (22), restrictively. Also, G_g and G_h are represented in (60) to estimate g and h functions. Thus, the error state trajectories asymptotically converge to zero.

Proof of Theorem 3 Define a Lyapunov function as

$$V_T = \frac{1}{2}z_1^2 + \frac{1}{2}z_2^2 + \frac{1}{2}z_3^2 + \frac{1}{2}\tilde{w}_g^T\tilde{w}_g + \frac{1}{2}\tilde{w}_h^T\tilde{w}_h \quad (70)$$

Differentiating (70) with respect to time is obtained as

$$\dot{V}_T = \underbrace{z_1\dot{z}_1}_{A} + \underbrace{z_2\dot{z}_2}_{B} + \underbrace{z_3\dot{z}_3}_{C} + \tilde{w}_g^T\dot{\tilde{w}}_g + \tilde{w}_h^T\dot{\tilde{w}}_h \quad (71)$$

Substituting (17) and (20) into A:

$$A = z_1\dot{z}_1 = -c_1z_1^2 \quad (72)$$

Substituting (23) into B:

$$B = z_2\dot{z}_2 = z_2\big(g(x_1,x_2) - \ddot{x}_{d\_1} + u_1(t) - \dot{\varphi}_1\big) \quad (73)$$

Let

$$u_1(t) = -c_2z_2 - \hat{g}(x_1,x_2) + \ddot{x}_{d\_1} + \dot{\varphi}_1 \quad (74)$$

Substituting (74) into (73), then B is obtained as

$$B = z_2\dot{z}_2 = -c_2z_2^2 + z_2\big[g(x_1,x_2) - \hat{g}(x_1,x_2)\big] \quad (75)$$

Let $g = w_g^{*T}G_g$ and $\hat{g} = \hat{w}_g^TG_g$, then

$$z_2\big[g(x_1,x_2) - \hat{g}(x_1,x_2)\big] = z_2\big(w_g^{*T} - \hat{w}_g^T\big)G_g = z_2\tilde{w}_g^TG_g \quad (76)$$

So,

$$B = z_2\dot{z}_2 = -c_2z_2^2 + z_2\tilde{w}_g^TG_g \quad (77)$$

Also, substituting (29) into C:

$$C = z_3\dot{z}_3 = z_3\big[h(x_1,x_2,x_3) - \dot{x}_{d\_3} + u_2(t)\big] \quad (78)$$

Let

$$u_2(t) = -c_3z_3 - \hat{h}(x_1,x_2,x_3) + \dot{x}_{d\_3} \quad (79)$$

Substituting (79) into (78), then C is obtained as

$$C = z_3\dot{z}_3 = -c_3z_3^2 + z_3\big[h(x_1,x_2,x_3) - \hat{h}(x_1,x_2,x_3)\big] \quad (80)$$

Let $h = w_h^{*T}G_h$ and $\hat{h} = \hat{w}_h^TG_h$. Then

$$z_3\big[h(x_1,x_2,x_3) - \hat{h}(x_1,x_2,x_3)\big] = z_3\big(w_h^{*T} - \hat{w}_h^T\big)G_h = z_3\tilde{w}_h^TG_h \quad (81)$$

So,

$$C = z_3\dot{z}_3 = -c_3z_3^2 + z_3\tilde{w}_h^TG_h \quad (82)$$

Substituting (72), (77), and (82) into (71), we obtain

$$\dot{V}_T = -c_1z_1^2 - c_2z_2^2 - c_3z_3^2 + \tilde{w}_g^T(z_2G_g + \dot{\tilde{w}}_g) + \tilde{w}_h^T(z_3G_h + \dot{\tilde{w}}_h) \quad (83)$$

IF the adaption laws are considered as follows:

$$\dot{\hat{w}}_g = -\dot{\tilde{w}}_g = z_2G_g \quad (84)$$

$$\dot{\hat{w}}_h = -\dot{\tilde{w}}_h = z_3G_h \quad (85)$$

Then the differentiation of Lyapunov function will be negative

$$\dot{V}_T = -c_1 z_1^2 - c_2 z_2^2 - c_3 z_3^2 < 0 \tag{86}$$

Therefore, the neural backstepping controllers designed in (66), (67) will asymptotically stabilize the system and the chaos control of unknown chaotic gyroscope system can be achieved. Also, the weights of GRBF$_{NN}$ identifiers will converge to optimal values. (Converging errors to zero are investigated in Appendix C.) □

7 GRBABC system to chaos synchronization of unknown chaotic gyroscope systems

The architecture of proposed method to chaos synchronization via Gaussian Radial Basis Adaptive Backstepping Control (*GRBABC*) system is shown in Fig. 8. The control laws of the GRBABC systems are developed as follows.

The neural backstepping controllers are chosen as follows to MPS of unknown chaotic gyroscope systems considered in (12):

$$u_1(t) = -k_1 e_2 - k_2 e_1 - (1-\alpha_1)\hat{p}(x_1, x_2, y_1, y_2, \alpha_1) \tag{87}$$

$$u_2(t) = -k_3 e_3 - (1-\alpha_2)\hat{q}(x_1, x_2, x_3, y_1, y_2, y_3, \alpha_2) \tag{88}$$

where two GRBF$_{NN}$ identifiers $\hat{p}$ and $\hat{q}$ are designed to online estimate the system dynamic functions p and q, restrictively. The following theorem shows the properties of the proposed GRBABC system to MPS of unknown chaotic gyroscope systems considered in (12).

Theorem 4 *Consider the MPS problem represented by* (12). *p and q are the unknown functions. The ideal control system is designed as* (36), (37). *The neural backstepping controller is designed as* (87), (88), *in which the adaptation laws of the GRBF$_{NN}$ identifiers are achieved as*

$$\dot{\hat{w}}_p = -\dot{\tilde{w}}_p = (1-\alpha_1) z_2 G_p \tag{89}$$

$$\dot{\hat{w}}_q = -\dot{\tilde{w}}_q = (1-\alpha_2) z_3 G_q \tag{90}$$

where z_2 and z_3 are represented in (44) *and* (50), *restrictively. $\alpha_1, \alpha_2 \in R$ are the scaling factors that define proportional relations between the synchronized systems.*

Thus, the trajectories of MPS error dynamics will converge to zero.

Proof of Theorem 4 Define a Lyapunov function as

$$V_T = \frac{1}{2} z_1^2 + \frac{1}{2} z_2^2 + \frac{1}{2} z_3^2 + \frac{1}{2} \tilde{w}_p^T \tilde{w}_p + \frac{1}{2} \tilde{w}_q^T \tilde{w}_q \tag{91}$$

Differentiating (91) with respect to time is obtained as

$$\dot{V}_T = \underbrace{z_1 \dot{z}_1}_{A} + \underbrace{z_2 \dot{z}_2}_{B} + \underbrace{z_3 \dot{z}_3}_{C} + \tilde{w}_p^T \dot{\tilde{w}}_p + \tilde{w}_q^T \dot{\tilde{w}}_q \tag{92}$$

Substituting (39) and (42) into A:

$$A = z_1 \dot{z}_1 = -c_1 z_1^2 \tag{93}$$

Substituting (45) into B:

$$\begin{aligned} B &= z_2 \dot{z}_2 \\ &= z_2 \left[(1-\alpha_1) p(x_1, x_2, y_1, y_2, \alpha_1) + u_1(t) - \dot{\varphi}_1 \right] \end{aligned} \tag{94}$$

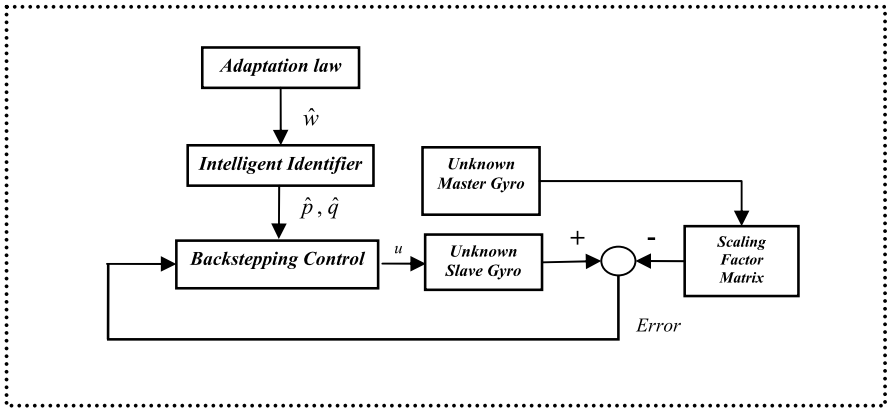

Fig. 8 Chaos synchronization via GRBABC system

Let

$$u_1(t) = -c_2 z_2 - (1-\alpha_1)\hat{p}(x_1, x_2, y_1, y_2, \alpha_1) + \dot{\varphi}_1 \tag{95}$$

Substituting (95) into (94), then B is obtained as

$$\begin{aligned} B &= z_2 \dot{z}_2 \\ &= -c_2 z_2^2 + (1-\alpha_1) z_2 \big[p(x_1, x_2, y_1, y_2, \alpha_1) \\ &\quad - \hat{p}(x_1, x_2, y_1, y_2, \alpha_1) \big] \end{aligned} \tag{96}$$

Let

$$p = w_p^{*T} G_p \quad \text{and} \quad \hat{q} = \hat{w}_q^T G_q$$

then

$$\begin{aligned} &\big[p(x_1, x_2, y_1, y_2, \alpha_1) - \hat{p}(x_1, x_2, y_1, y_2, \alpha_1) \big] \\ &\quad = z_2 \big(w_p^{*T} - \hat{w}_p^T \big) G_p = z_2 \tilde{w}_p^T G_p \end{aligned} \tag{97}$$

So,

$$B = z_2 \dot{z}_2 = -c_2 z_2^2 + (1-\alpha_1) z_2 \tilde{w}_p^T G_p \tag{98}$$

Also, substituting (51) into C:

$$\begin{aligned} C &= z_3 \dot{z}_3 \\ &= z_3 \big[(1-\alpha_2) q(x_1, x_2, x_3, y_1, y_2, y_3, \alpha_2) + u_2(t) \big] \end{aligned} \tag{99}$$

Let

$$u_2(t) = -c_3 z_3 - (1-\alpha_2)\hat{q}(x_1, x_2, x_3, y_1, y_2, y_3, \alpha_2) \tag{100}$$

Substituting (100) into (99), then C is obtained as

$$\begin{aligned} C &= z_3 \dot{z}_3 \\ &= -c_3 z_3^2 + (1-\alpha_2) z_3 \big[q(x_1, x_2, x_3, y_1, y_2, y_3, \alpha_2) \\ &\quad - \hat{q}(x_1, x_2, x_3, y_1, y_2, y_3, \alpha_2) \big] \end{aligned} \tag{101}$$

Let

$$q = w_q^{*T} G_q \quad \text{and} \quad \hat{q} = \hat{w}_q^T G_q$$

then

$$\begin{aligned} &\big[q(x_1, x_2, x_3, y_1, y_2, y_3, \alpha_2) \\ &\quad - \hat{q}(x_1, x_2, x_3, y_1, y_2, y_3, \alpha_2) \big] \\ &= \big(w_q^{*T} - \hat{w}_q^T \big) G_q = \tilde{w}_q^T G_q \end{aligned} \tag{102}$$

So,

$$C = z_3 \dot{z}_3 = -c_3 z_3^2 + (1-\alpha_2) z_3 \tilde{w}_q^T G_q \tag{103}$$

Substituting (93), (98), and (103) into (92):

$$\begin{aligned} \dot{V}_T = &-c_1 z_1^2 - c_2 z_2^2 - c_3 z_3^2 \\ &+ \tilde{w}_p^T \big[(1-\alpha_2) z_2 G_p + \dot{\tilde{w}}_p \big] \\ &+ \tilde{w}_q^T \big[(1-\alpha_2) z_3 G_q + \dot{\tilde{w}}_q \big] \end{aligned} \tag{104}$$

If the adaption laws are considered as follows:

$$\dot{\hat{w}}_p = -\dot{\tilde{w}}_p = (1-\alpha_1) z_2 G_p \tag{105}$$

$$\dot{\hat{w}}_q = -\dot{\tilde{w}}_q = (1-\alpha_2) z_3 G_q \tag{106}$$

Then the differentiation of Lyapunov function will be negative.

$$\dot{V}_T = -c_1 z_1^2 - c_2 z_2^2 - c_3 z_3^2 < 0 \tag{107}$$

Therefore, the neural backstepping controllers designed in (87), (88) will asymptotically stabilize the system and the MPS of unknown chaotic gyroscope systems can be achieved. Also, the weights of GRBF_{NN} identifiers will converge to optimal values. □

8 Novelty of GRBABC system

For some systems, since the dynamic characteristics of the control system are nonlinear and the precise models are difficult to obtain, the model-based control approaches are difficult to be implemented. To overcome this drawback, a novel Gaussian radial basis adaptive backstepping control (GRBABC) system has been proposed. In the neural nonlinear controller, a GRBF_{NN} identifier is utilized to estimate the system dynamic function in an online manner. The adaptive law of the GRBABC system is synthesized using the Lyapunov functions so that the asymptotic stability of the control system can be guaranteed.

The GRBABC system to chaos control and MPS is shown in Figs. 9 and 10, respectively. Figures 9 and 10 are two flowcharts that explain how the GRBABC system can be used for chaos control and modified projective synchronization.

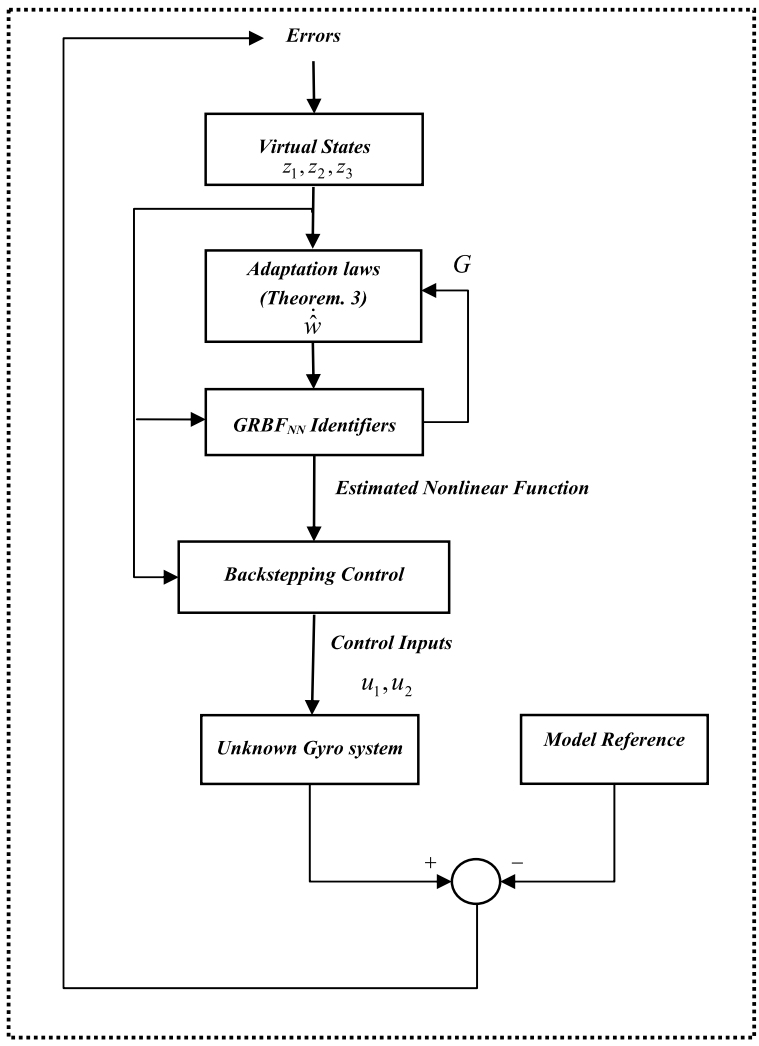

Fig. 9 The GRBABC system to chaos control of chaotic gyroscope system

Suppression of the chaos is presented so as to improve the performance of a dynamical system. To achieve modified projective synchronization (MPS), it is clear that the proposed methods are capable to create a full range MPS of all state variables in a proportional way. The proposed method allows us to arbitrarily adjust the desired scaling by controlling the slave system, but the complete synchronization is not considered in the proposed method. It is not necessary to calculate the Lyapunov exponents and the eigenvalues of the Jacobian matrix, which makes it simple and convenient. Also, it is a systematic procedure for MPS of chaotic systems and it can be applied to a variety of chaotic systems no matter whether it contains external excitation or not. Notice that it needs only one controller to realize MPS no matter how many dimensions the chaotic system contains and the controller is easy to implement.

In the next section, simulation results are presented to show the effectiveness of the proposed method for chaos control and synchronization of known and unknown chaotic gyroscope systems.

9 Simulation results

In this section, numerical simulations are given to demonstrate chaos control and MPS of the known and unknown nonlinear heavy symmetric gyroscope systems via GRBABC. The parameters of nonlinear gyros

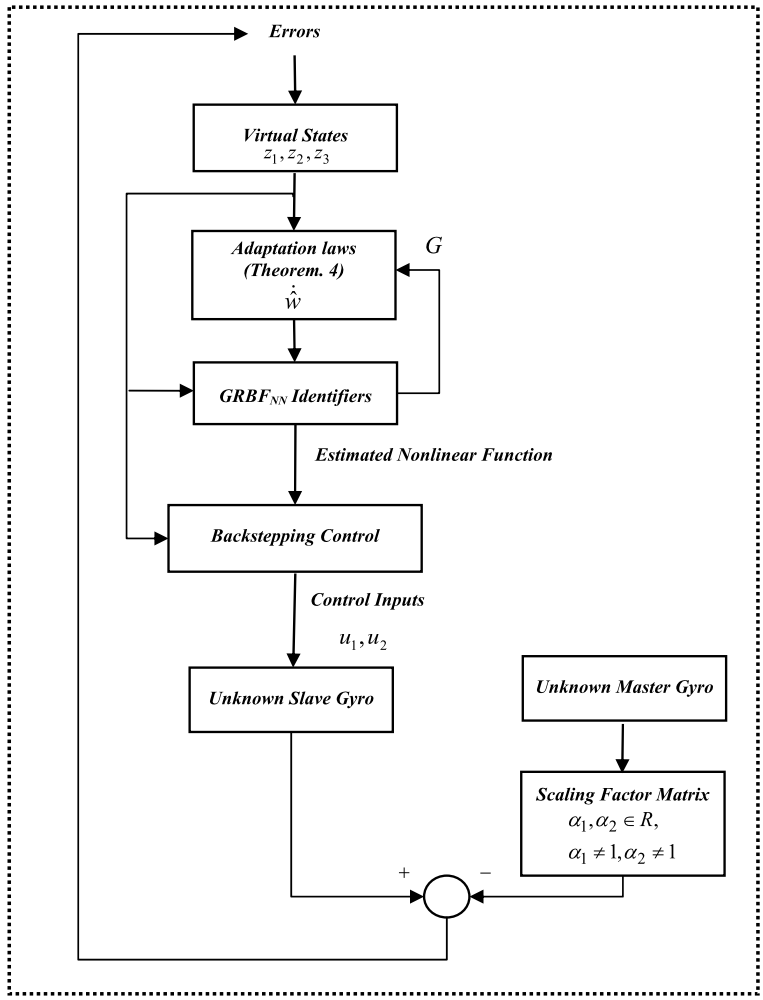

Fig. 10 The GRBABC system to MPS of chaotic gyroscope systems

systems are specified as follows:

$$\beta_\phi = 2, \quad \beta_\psi = 5, \quad l = 0.25, \quad I_1 = 1$$
$$M_g = 4, \quad c_1 = 0.5, \quad \omega = 2, \quad A = 50$$

which, as shown in Sect. 2, give rise to a chaotic state.

9.1 Simulation results of chaos control via ideal backstepping control (Theorem 1)

Numerical simulations are given to demonstrate tracking control of the nonlinear gyro to two desired trajectories: regular and periodic trajectories. Regular trajectories are defined as

$$X_{d\_\text{Regular}}(t) = \left[\frac{\pi}{3}, 0, 1\right]^T$$

and periodic trajectories are defined as follows:

$$X_{d\_\text{Periodic}}(t) = \begin{bmatrix} k\cos(wt) + d_1 \\ -kw\sin(wt) \\ k\sin(wt) + d_2 \end{bmatrix}$$

where $k = 1$, $w = 1$, and $d_1 = d_2 = 1.5$. The initial conditions are defined as

$$\left[x_1(0)\ x_2(0)\ x_3(0)\right]^T = [1\ -1\ -1]^T$$

The time responses of the nonlinear gyroscope controlled to track regular trajectories are shown in Fig. 11, and the corresponding error states converge asymptotically to zero in Fig. 12. The corresponding control inputs are shown in Fig. 13.

The time responses of the nonlinear gyroscope controlled with track periodic trajectories are

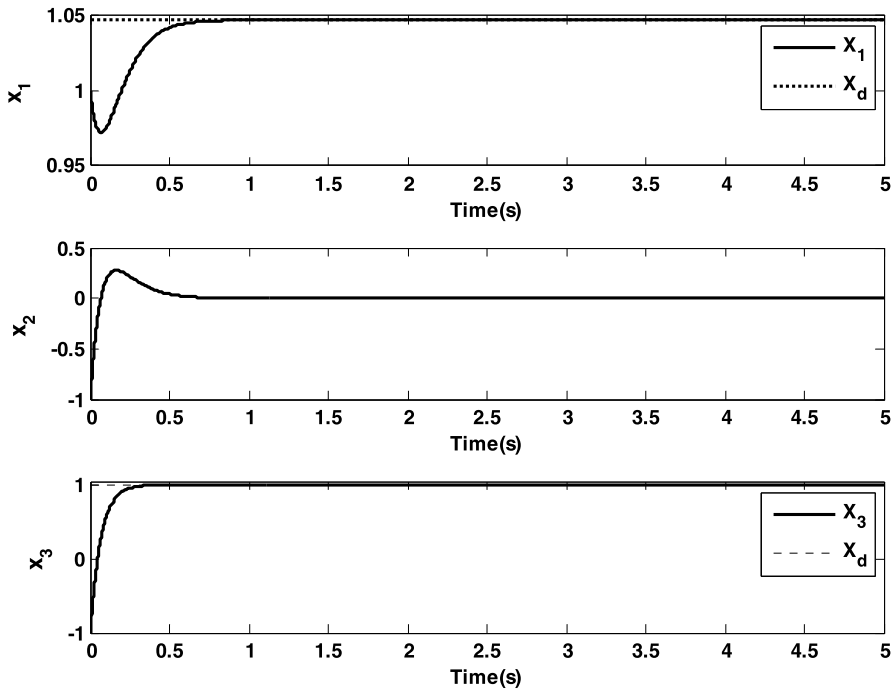

Fig. 11 Control via ideal backstepping control: time responses of state variables (tracking regular trajectories). Trajectories of state variables and desired states are shown with *solid* and *dashed line*, respectively

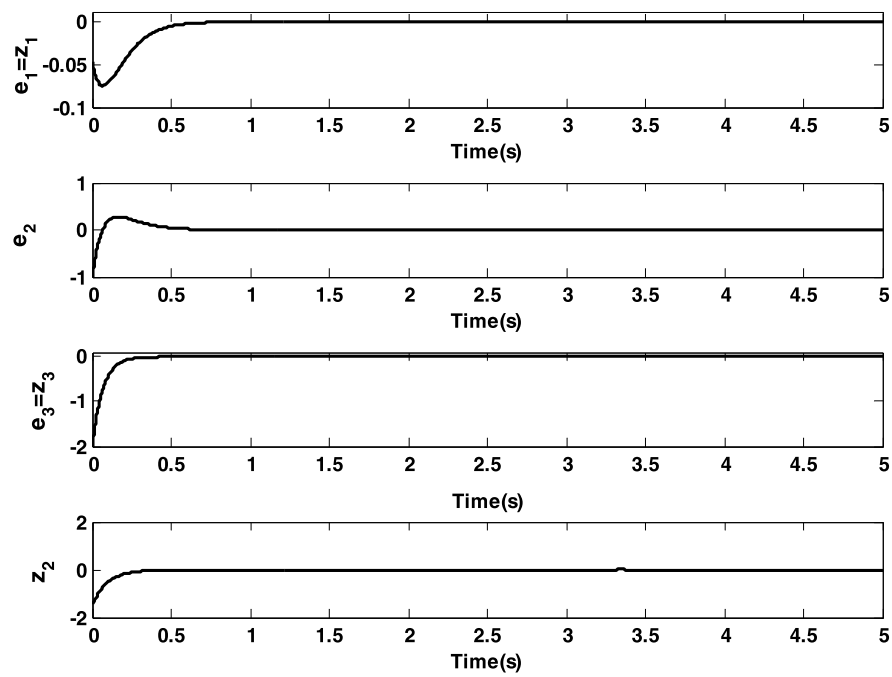

Fig. 12 Control via ideal backstepping control: time response of tracking error states and virtual states (tracking regular trajectories)

shown in Fig. 14, where the corresponding error states converge asymptotically to zero in Fig. 15. The corresponding control inputs are shown in Fig. 16.

The simulation results of chaos control of nonlinear gyro via ideal backstepping control have good performances and confirm that the error states are asymptotically regulated to zero.

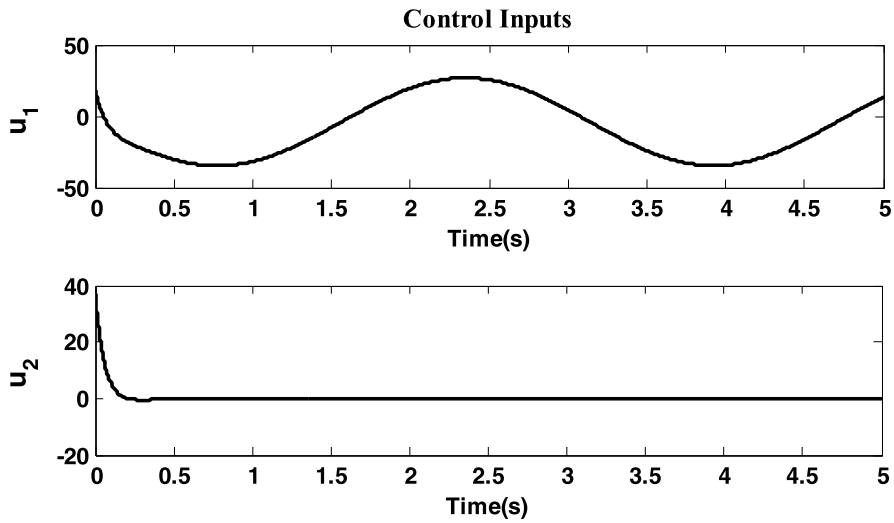

Fig. 13 Control via ideal backstepping control: control inputs (tracking regular trajectories)

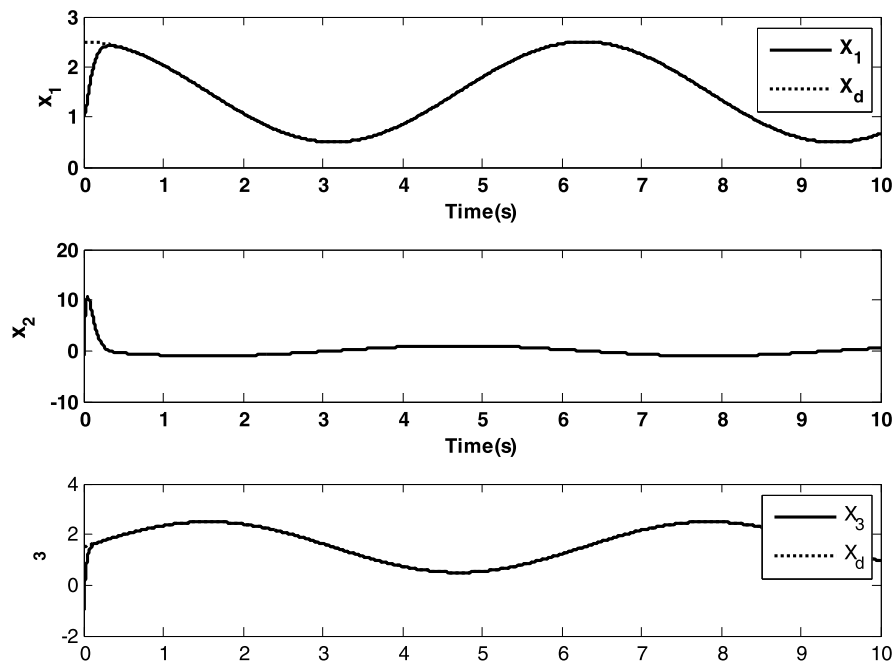

Fig. 14 Control via ideal backstepping control: time responses of state variables (tracking periodic trajectories). trajectories of state variables and desired states are shown with *solid* and *dashed line*, respectively

9.2 Simulation results of MPS via ideal backstepping control (Theorem 2)

Numerical simulations are given to demonstrate MPS of the chaotic nonlinear gyros via ideal backstepping control.

The scaling factor is specified as $\alpha_2 = 0.5$, $\alpha_2 = -0.5$ and the initial conditions are defined as

$$\left[x_1(0)\ x_2(0)\ x_3(0)\right]^T = [1\ -1\ 1]^T,$$
$$\left[y_1(0)\ y_2(0)\ y_3(0)\right]^T = [2\ 2\ -2]^T$$

The time responses of controlled master-slave chaotic gyros are shown in Fig. 17. Obviously, the MPS errors converge asymptotically to zero in Fig. 18. The corresponding control inputs are shown in Fig. 19.

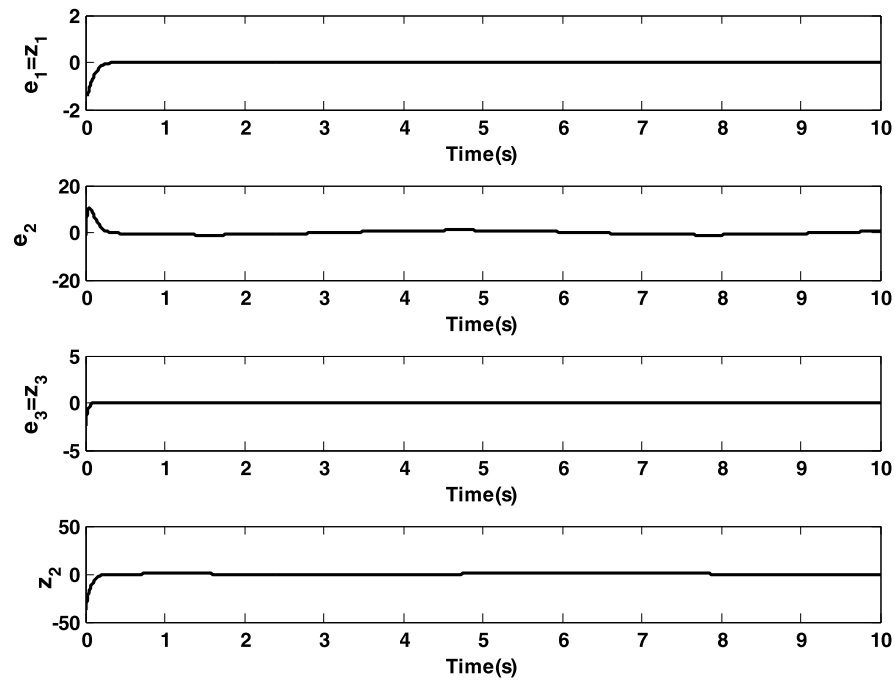

Fig. 15 Control via ideal backstepping control: time response of tracking error states (tracking periodic trajectories)

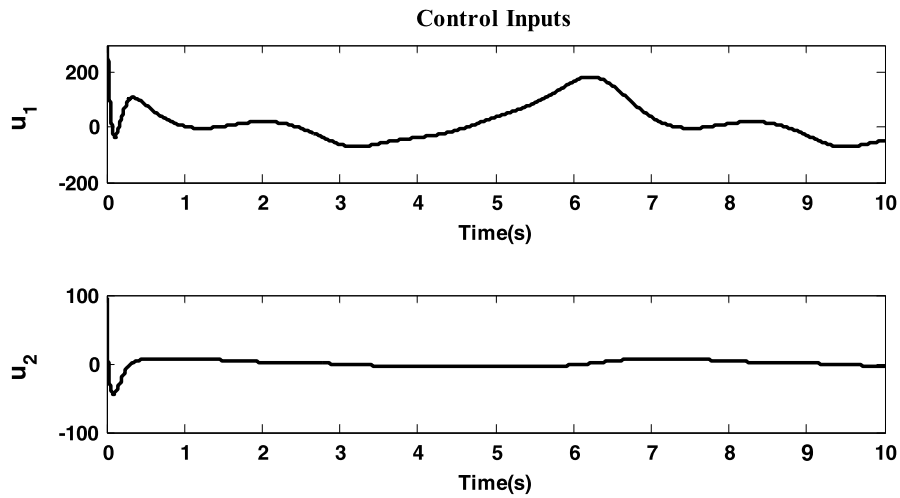

Fig. 16 Control via ideal backstepping control: control inputs (tracking periodic trajectories)

The simulation results of MPS via ideal backstepping control have good performances and confirm that the master and slave systems achieve the modified projective synchronized states. Also, these results demonstrate that the system error states are asymptotically regulated to zero.

9.3 Simulation results of chaos control via GRBABC (Theorem 3)

Assume that the dynamic functions of the chaotic gyroscope are unknown. The system dynamic function would be estimated online by two GRBF_{NN} identifiers. The GRBF_{NN} identifiers with five hidden nodes are utilized to approach the system dynamic functions of the chaotic gyroscope system.

Numerical simulations are given to demonstrate the tracking control of the unknown chaotic gyro to two desired trajectories: Regular and periodic trajectories. Regular trajectories are defined as:

$$X_{d\_\text{Regular}}(t) = \left[\frac{\pi}{3}, 0, 1\right]^T$$

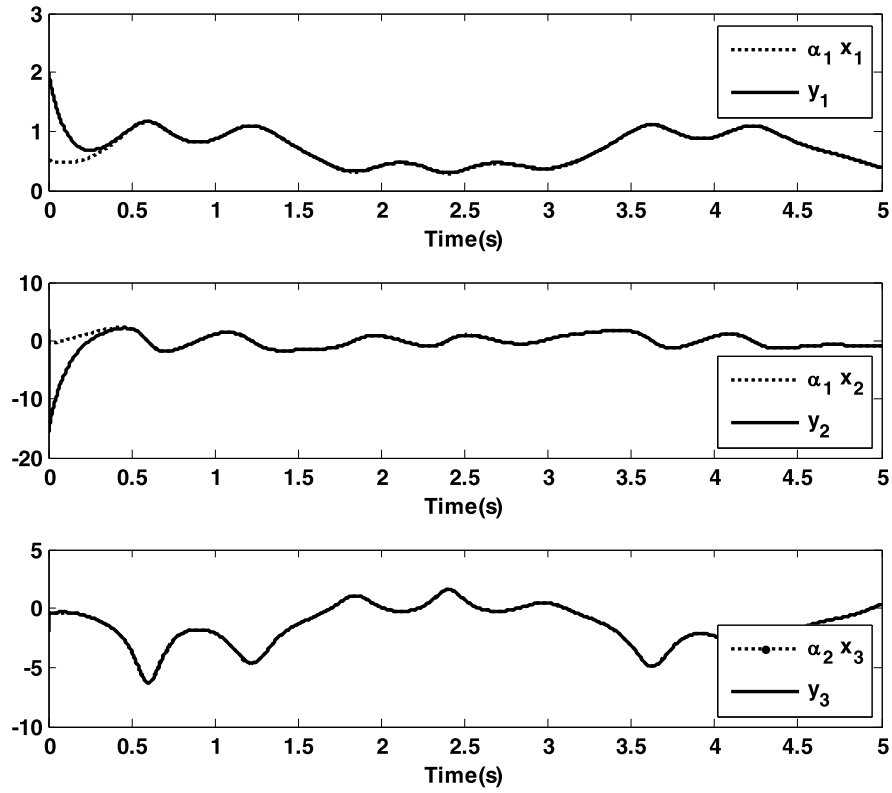

Fig. 17 MPS via ideal backstepping control: time response of state variables

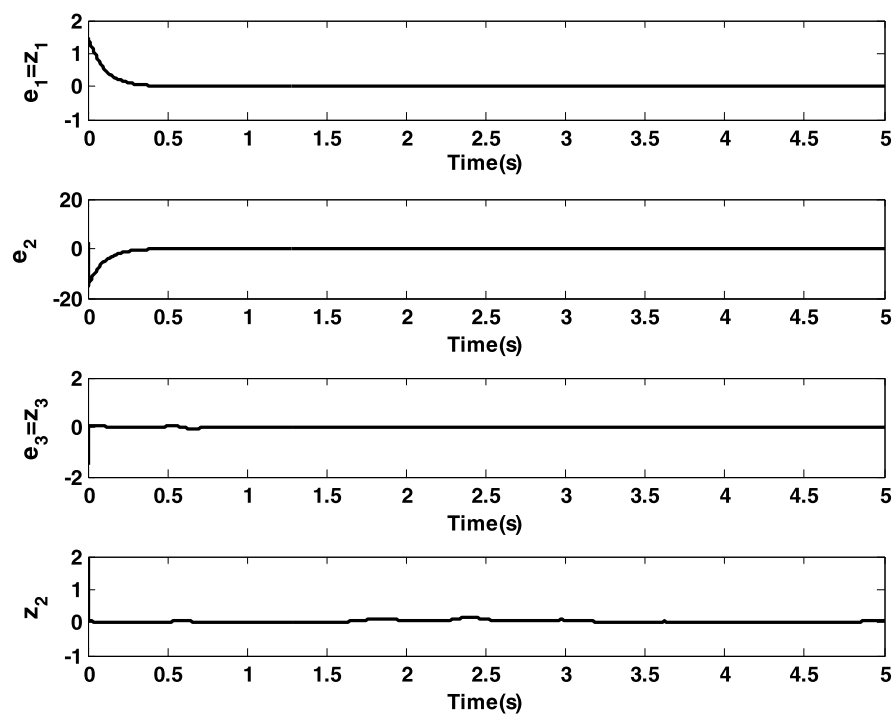

Fig. 18 MPS via ideal backstepping control: time response of MPS error states and virtual states

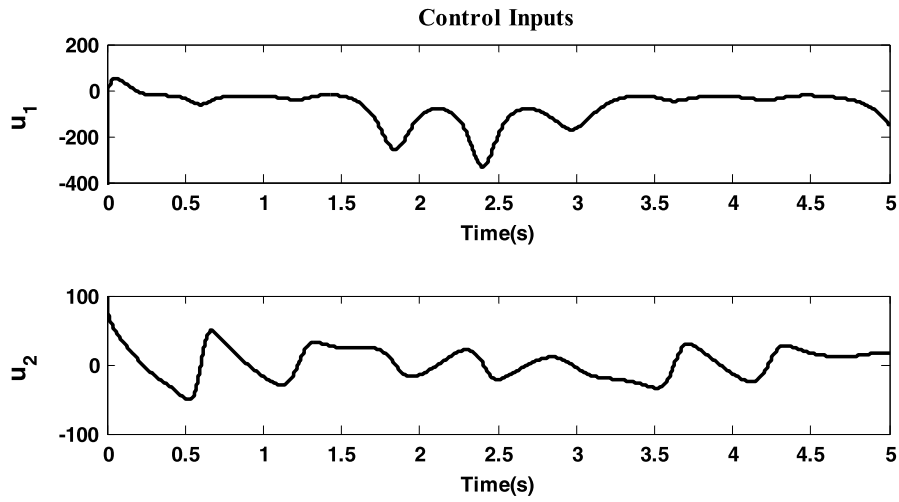

Fig. 19 MPS via ideal backstepping control: control inputs

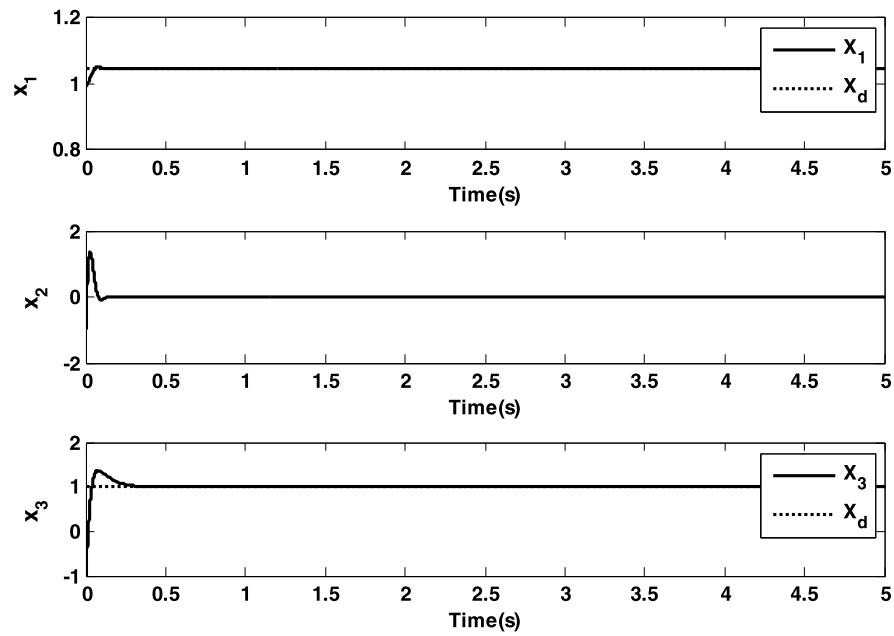

Fig. 20 Control of unknown chaotic gyroscope via GRBABC: time responses of state variables (tracking regular trajectories). Trajectories of state variables and desired states are shown with *solid* and *dashed line*, respectively

and periodic trajectories are defined as follows:

$$X_{d\_\text{Periodic}}(t) = \begin{bmatrix} k\cos(wt) + d_1 \\ -kw\sin(wt) \\ k\sin(wt) + d_2 \end{bmatrix}$$

where $k = 1$, $w = 1$ and $d_1 = d_2 = 1.5$.

The initial conditions are defined as

$$\begin{bmatrix} x_1(0)\ x_2(0)\ x_3(0) \end{bmatrix}^T = [1\ -1\ 1]^T$$

The time responses of the unknown chaotic gyroscope controlled to track regular trajectories are shown in Fig. 20, and the corresponding error states asymptotically to zero in Fig. 21. The corresponding control inputs are shown in Fig. 22.

The time responses of the nonlinear gyroscope controlled with track periodic trajectories are shown in Fig. 23, where the corresponding error states converge asymptotically to zero in Fig. 24. The corresponding control inputs are shown in Fig. 25.

The simulation results of chaos control of unknown chaotic gyroscope via GRBABC have good performances and confirm that the error states are asymptotically regulated to zero.

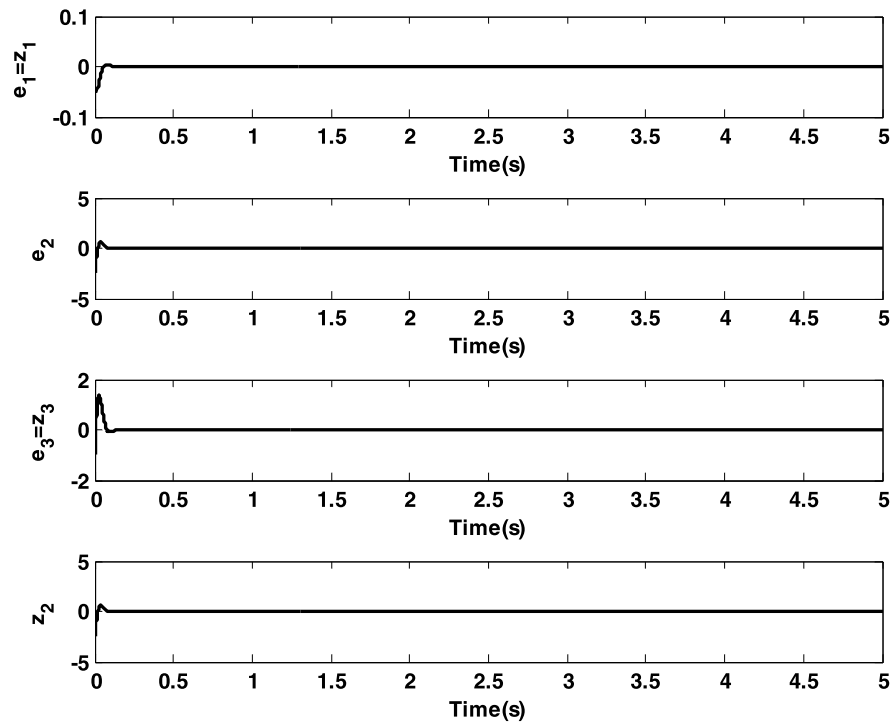

Fig. 21 Control of unknown chaotic gyroscope via GRBABC: time response of tracking error states and virtual states (tracking regular trajectories)

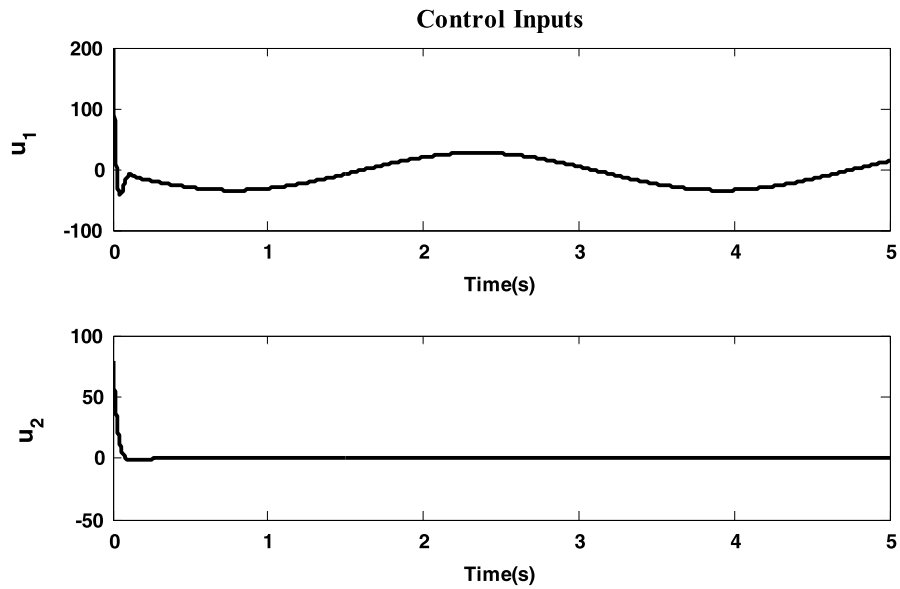

Fig. 22 Control of unknown chaotic gyroscope via GRBABC: control inputs (tracking regular trajectories)

9.4 Simulation results of MPS via GRBABC (Theorem 4)

Assuming that the dynamic functions of chaotic gyroscope are unknown, the system dynamic functions would be estimated online by two GRBF_{NN} identifiers. The GRBF_{NN} identifiers with five hidden nodes are utilized to approach the system dynamic functions of the chaotic system.

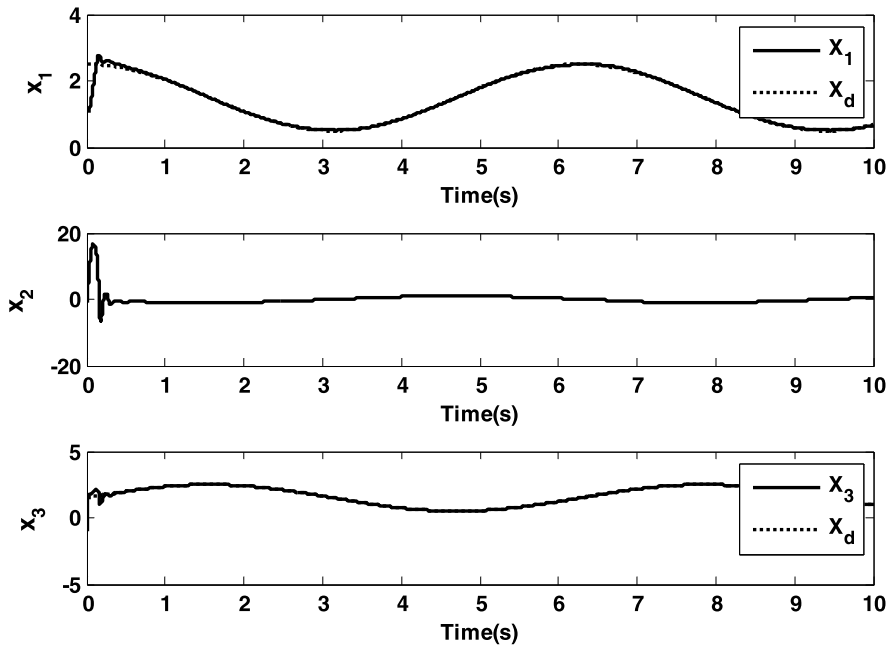

Fig. 23 Control of unknown chaotic gyroscope via GRBABC: time responses of state variables (tracking periodic trajectories). Trajectories of state variables and desired states are shown with *solid* and *dashed line*, respectively

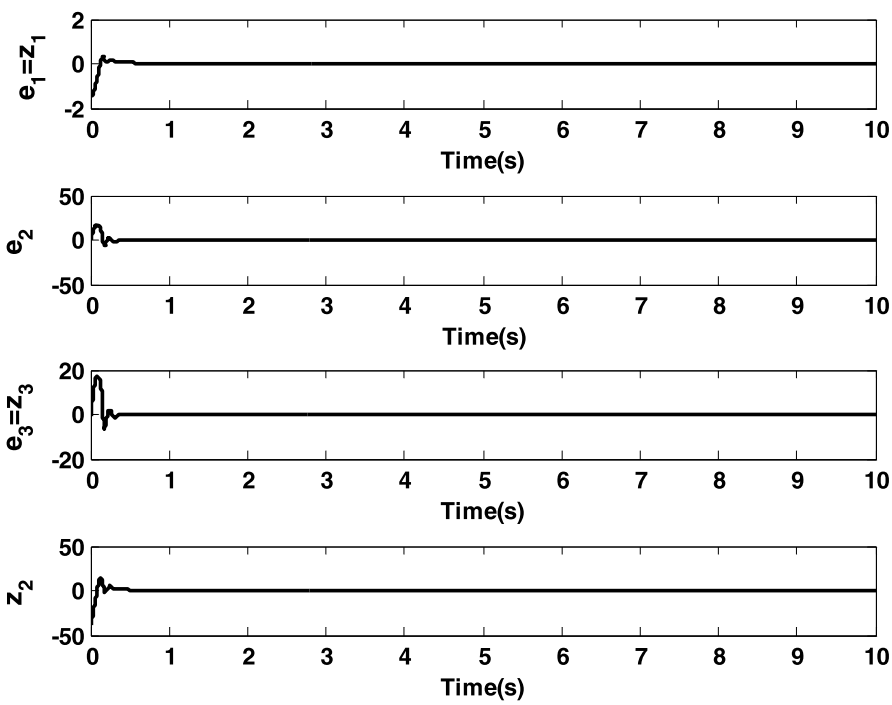

Fig. 24 Control of unknown chaotic gyroscope via GRBABC: time response of tracking error states and virtual states (tracking periodic trajectories)

Numerical simulations are given to demonstrate MPS of the chaotic nonlinear gyros via GRBABC.

The scaling factor is specified as $\alpha_1 = 0.5$, $\alpha_2 = -0.5$ and the initial conditions are defined as

$$\left[x_1(0)\ x_2(0)\ x_3(0)\right]^T = [1\ -1\ 1]^T$$

$$\left[y_1(0)\ y_2(0)\ y_3(0)\right]^T = [2\ 2\ -2]^T$$

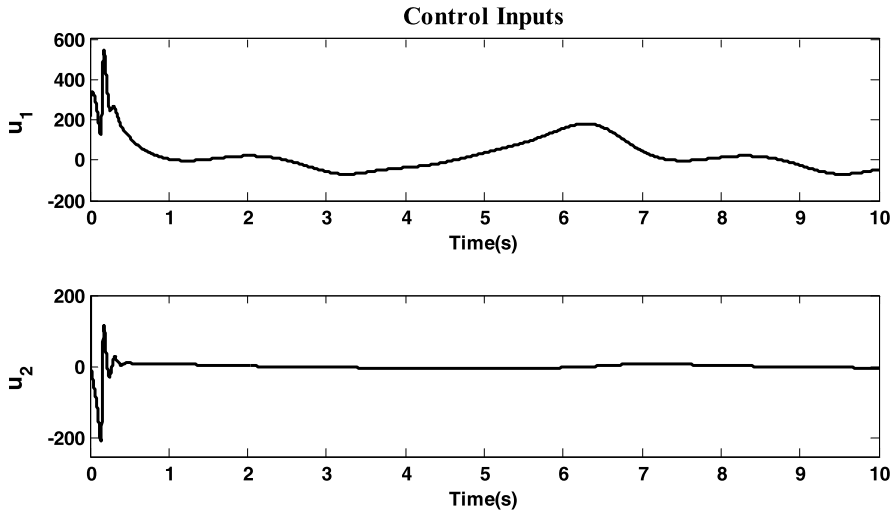

Fig. 25 Control of unknown chaotic gyroscope via GRBABC: control inputs (tracking periodic trajectories)

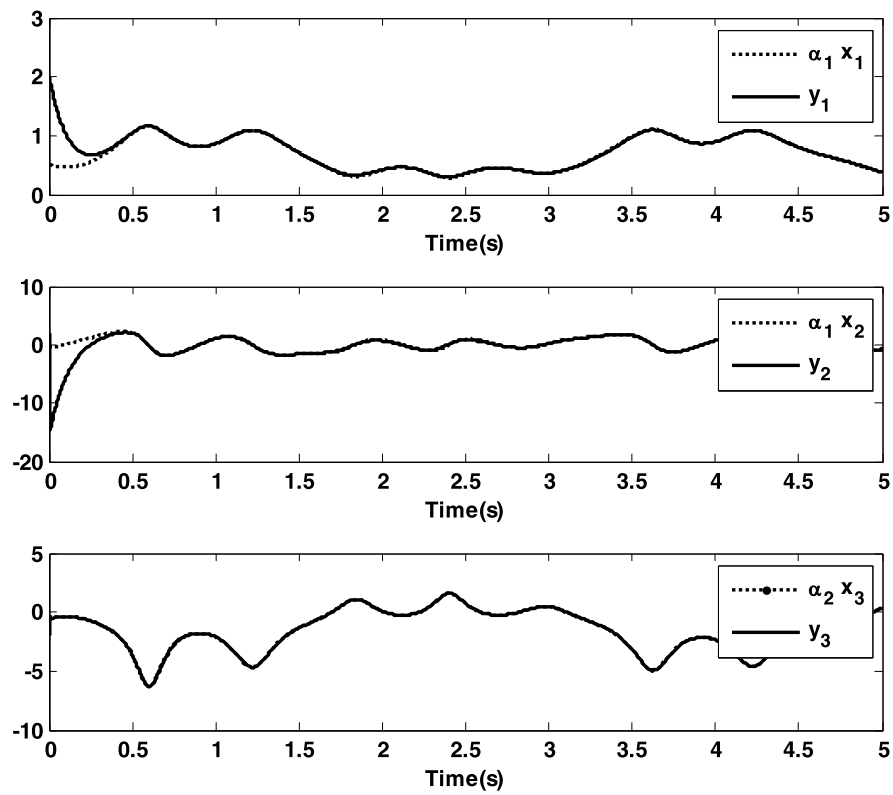

Fig. 26 MPS of unknown chaotic gyros via GRBABC: time response of state variables

The time responses of controlled master-slave chaotic gyros are shown in Fig. 26. Obviously, the MPS errors converge asymptotically to zero in Fig. 27. The corresponding control inputs are shown in Fig. 28.

The simulation results of MPS via GRBABC have good performances and confirm that the master and slave systems achieve the modified projective synchronized states. Also, these results demonstrate that

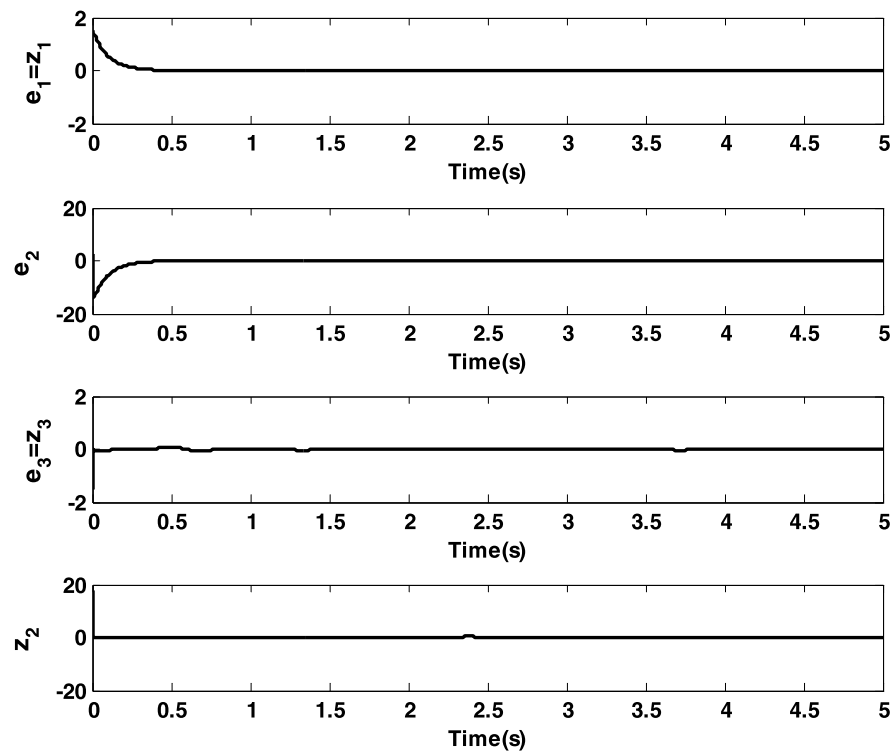

Fig. 27 MPS of unknown chaotic gyros via GRBABC: time response of MPS error states

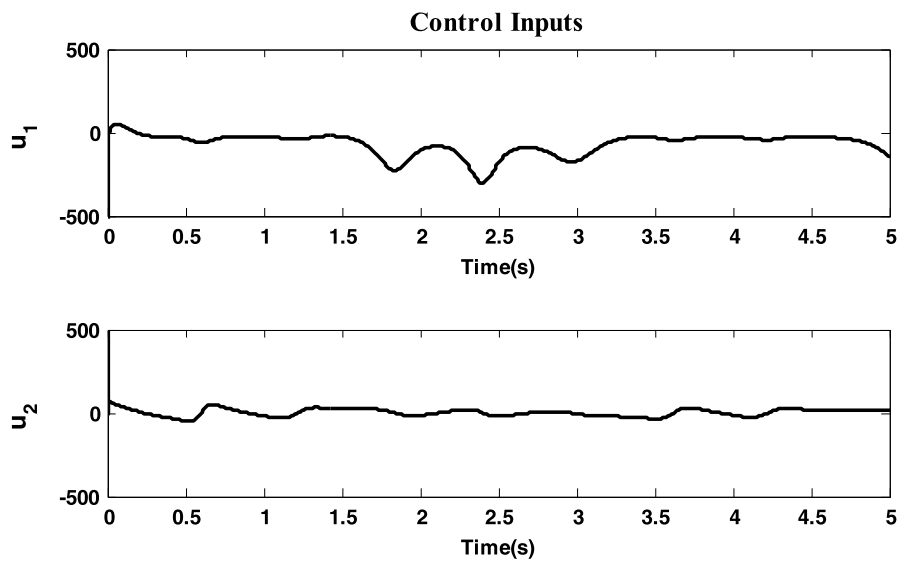

Fig. 28 MPS of unknown chaotic gyros via GRBABC: control inputs

the system error states are asymptotically regulated to zero.

10 Conclusion

In this paper, the chaos control and MPS of unknown heavy symmetric chaotic gyroscope systems via Gaussian radial basis adaptive backstepping control are studied.

Since for some systems, the dynamic characteristics of the control system are nonlinear and the precise models are difficult to obtain, the model-based control approaches are difficult to be implemented. To

overcome this drawback, a novel GRBABC system has been proposed. In the neural nonlinear controller, a GRBF_{NN} identifier is utilized to estimate the system dynamic function in an online manner. The adaptive law of the GRBABC system is synthesized using the Lyapunov functions so that the asymptotic stability of the control system can be guaranteed.

Suppression of the chaos is presented so as to improve the performance of a dynamical system. To achieve MPS, it is clear that the proposed methods are capable to create a full range MPS of all state variables in a proportional way. It also allows us to arbitrarily adjust the desired scaling by controlling the slave system, but the complete synchronization is not considered in the proposed method. It is not necessary to calculate the Lyapunov exponents and the eigenvalues of the Jacobian matrix, which makes it simple and convenient.

The advantages of the Gaussian radial basis adaptive backstepping control can be summarized as follows:

(1) It is a systematic procedure for control and synchronization of uncertain chaotic systems.
(2) It can be applied to a variety of chaotic systems no matter whether it contains external excitation or not.
(3) It needs only one control system to realize chaos control and synchronization no matter how much dimensions the chaotic system contains.
(4) The controller is easy to be implemented.

The proposed techniques have been successfully applied to unknown heavy symmetric chaotic gyroscope systems. Simulations results show that the proposed method is very effective and robust against system uncertainty.

Since the gyro has been utilized to describe the mode in navigational, aeronautical or space engineering, the chaos control and MPS procedure of chaotic gyroscope systems in this study may have practical applications in the future.

Appendix A: Modeling of chaotic symmetric gyroscope

The symmetric gyroscope mounted on a vibrating base is shown in Fig. 1. The dynamics of a heavy symmetric gyroscope with linear-plus-cubic damping of angle θ mounted on a vibrating base can be described by Euler's angels θ (nutation), ϕ (precession), and ψ (spin). The Lagrangian can be written as follows [24, 25]:

$$L = \frac{1}{2}I_1\left(\dot{\theta}^2 + \dot{\phi}^2\sin^2\theta\right) + \frac{1}{2}I_3(\dot{\phi}\cos\theta + \dot{\psi})^2 - M_g(l + A\sin\omega t)\cos\theta \tag{A.1}$$

where I_1 and I_3 are the polar and equatorial moments of inertia of symmetric gyro, respectively.

M_g is the gravity force, l the amplitude of the external excitation disturbance, and ω is the frequency of the external excitation disturbance. Coordinates ϕ and ψ are cyclic, as they are absent from the Lagrangian, which provides us with two first integrals of the motion expressing the conjugate momenta. The momentum integrals are [24, 25]:

$$P_\phi = \frac{\partial L}{\partial\dot{\phi}} = I_1\dot{\phi}\sin^2\theta + I_3(\dot{\phi}\cos\theta + \dot{\psi})\cos\theta = \beta_\phi \tag{A.2}$$

$$P_\psi = \frac{\partial L}{\partial\dot{\psi}} = I_3(\dot{\phi}\cos\theta + \dot{\psi}) = I_3\omega_z = \beta_\psi \tag{A.3}$$

where ω_z is the spin velocity of the gyro. The Routh's procedure is adopted along with the above-mentioned relations, the Routhian of the system becomes:

$$R = L - \beta_\phi\dot{\phi} - \beta_\psi\dot{\psi} = \frac{1}{2}I_1\dot{\theta}^2 - \left[\frac{(\beta_\phi - \beta_\psi\cos\theta)^2}{2I_1\sin^2\theta} + \frac{\beta_\phi^2}{2I_3} + M_g(l + A\sin\omega t)\cos\theta\right] \tag{A.4}$$

The equation above depends on the angle θ alone. According to [25], $\beta_\phi = \beta_\psi$ when $\theta = 0$. The dissipative force is also assumed to be in linear form as

$$F = -c_1\dot{\theta} \tag{A.5}$$

where c_1 is positive constants.

The equations of motion describing the system can be obtained from:

$$\frac{d}{dt}\left(\frac{\partial R}{\partial\dot{\theta}}\right) - \frac{\partial R}{\partial\theta} = F \tag{A.6}$$

$$\frac{d}{dt}\left(\frac{\partial R}{\partial\dot{\phi}}\right) - \frac{\partial R}{\partial\phi} = 0 \tag{A.7}$$

The equations governing the gyroscope are given as

$$\ddot{\theta} + \frac{(\beta_\phi - \beta_\psi \cos\theta)(B_\psi - \beta_\phi \cos\theta)}{I_1^2 \sin^3\theta} + \frac{c_1}{I_1}\dot{\theta} - \frac{M_g l}{I_1}\sin\theta + \frac{M_g A}{I_1}\sin(\omega t)\sin\theta = 0 \tag{A.8}$$

$$\ddot{\phi} + 2\dot{\phi}\dot{\theta}\frac{\cos\theta}{\sin\theta} - \frac{\beta_\psi}{I_1 \sin\theta}\dot{\theta} = 0 \tag{A.9}$$

Notice that with considering $\frac{d}{dt}(\frac{\partial R}{\partial \dot{\psi}}) - \frac{\partial R}{\partial \psi} = 0$, we obtain B_ψ is constant. According to (A.3), $\beta_\psi = I_3\omega_z$, it is correct for the coordinate ψ.

Therefore, (A.8) and (A.9) are the differential equations governing the chaotic symmetric gyroscope system. Let the state variables $x = [\theta\ \dot{\theta}\ \dot{\phi}]^T$, then the dynamic equations can be obtained as

$$\begin{cases} \dot{x}_1 = x_2 \\ \dot{x}_2 = -\dfrac{(\beta_\phi - \beta_\psi \cos x_1)(B_\psi - \beta_\phi \cos x_1)}{I_1^2 \sin^3 x_1} - \dfrac{c_1}{I_1}x_2 + \dfrac{M_g l}{I_1}\sin x_1 - \dfrac{M_g A}{I_1}\sin\omega t \sin x_1 \\ \dot{x}_3 = -2x_2x_3\dfrac{\cos x_1}{\sin x_1} + \dfrac{\beta_\psi}{I_1 \sin x_1}x_2 \end{cases} \tag{A.10}$$

Equation (A.10) is presented in Sect. 2 as (1).

Appendix B: Investigation of converging errors to zero for Theorem 1

Equations (14) and (15), the designed control inputs, must be substituted in (6) as follows:

$$\begin{cases} \dot{e}_1 = e_2 \\ \dot{e}_2 = -k_1e_2 - k_2e_1 \\ \dot{e}_3 = -k_3e_3 \end{cases} \tag{B.1}$$

So,

$$\begin{aligned} &\ddot{e}_1 = \dot{e}_2 = -k_1e_2 - k_2e_1 = -k_1\dot{e}_1 - k_2e_1 \quad \Rightarrow \\ &\quad \ddot{e}_1 + k_1\dot{e}_1 + k_2e_1 = 0 \\ &\ddot{e}_2 = -k_1\dot{e}_2 - k_2\dot{e}_1 = -k_1\dot{e}_2 - k_2e_2 \quad \Rightarrow \\ &\quad \ddot{e}_2 + k_1\dot{e}_2 + k_2e_2 = 0 \\ &\dot{e}_3 = -k_3e_3 \quad \Rightarrow \quad \dot{e}_3 + k_3e_3 = 0 \\ &\downarrow \\ &\begin{cases} \ddot{e}_1 + k_1\dot{e}_1 + k_2e_1 = 0 \\ \ddot{e}_2 + k_1\dot{e}_2 + k_2e_2 = 0 \\ \dot{e}_3 + k_3e_3 = 0 \end{cases} \end{aligned} \tag{B.2}$$

Then three differential equations are obtained that they are exponential stable. After solving them, we obtain

$$\begin{cases} e_1(t) = a_1e^{(\frac{-k_1+\sqrt{k_1^2-4k_2}}{2})t} + a_2e^{(\frac{-k_1-\sqrt{k_1^2-4k_2}}{2})t} \\ e_2(t) = a_3e^{(\frac{-k_1+\sqrt{k_1^2-4k_2}}{2})t} + a_4e^{(\frac{-k_1-\sqrt{k_1^2-4k_2}}{2})t} \\ e_3(t) = a_5e^{-k_3t} \end{cases} \tag{B.3}$$

Notice, k_1, k_2, k_3 are positive constant parameters. If $k_1 > 2\sqrt{k_2}$, then $(k_1^2 - 4k_2)$ is positive. When $t \to \infty$, then

$$\begin{cases} \lim\limits_{t\to\infty} e_1(t) \to 0 \\ \lim\limits_{t\to\infty} e_2(t) \to 0 \\ \lim\limits_{t\to\infty} e_3(t) \to 0 \end{cases} \tag{B.4}$$

Therefore, the tracking trajectory is achieved.

Appendix C: Investigation of converging errors to zero for Theorem 3

The same considerations as the previous Appendix, (66) and (67), the designed control inputs, must be substituted in (6) as follows:

$$\begin{cases} \dot{e}_1 = e_2 \\ \dot{e}_2 = -k_1e_2 - k_2e_1 + \left[g(x_1, x_2) - \hat{g}(x_1, x_2)\right] \\ \dot{e}_3 = -k_3e_3 + \left[h(x_1, x_2, x_3) - \hat{h}(x_1, x_2, x_3)\right] \end{cases} \tag{C.1}$$

where two GRBF_{NN} identifiers $\hat{g}$ and $\hat{h}$ are designed to online estimate the system dynamic functions g and h, restrictively.

Let $g = w_g^{*T} G_g$ and $\hat{g} = \hat{w}_g^T G_g$, as mentioned before (76), then

$$\left[g(x_1, x_2) - \hat{g}(x_1, x_2)\right] = \left(w_g^{*T} - \hat{w}_g^T\right) G_g = \tilde{w}_g^T G_g \tag{C.2}$$

Also, let $h = w_h^{*T} G_h$ and $\hat{h} = \hat{w}_h^T G_h$, as mentioned before (81), then

$$\begin{aligned}&\left[h(x_1, x_2, x_3) - \hat{h}(x_1, x_2, x_3)\right]\\ &\quad = \left(w_h^{*T} - \hat{w}_h^T\right) G_h = \tilde{w}_h^T G_h\end{aligned} \tag{C.3}$$

From the two previous equations, (6) can be rewritten as follows:

$$\begin{cases} \dot{e}_1 = e_2 \\ \dot{e}_2 = -k_1 e_2 - k_2 e_1 + \left[g(x_1, x_2) - \hat{g}(x_1, x_2)\right] \\ \quad = -k_1 e_2 - k_2 e_1 + \tilde{w}_g^T G_g \\ \dot{e}_3 = -k_3 e_3 + \left[h(x_1, x_2, x_3) - \hat{h}(x_1, x_2, x_3)\right] \\ \quad = -k_3 e_3 + \tilde{w}_h^T G_h \end{cases} \tag{C.4}$$

With considering the Lyapunov function (defined in proof of Theorem 3 in previous version of paper) as

$$V_T = \frac{1}{2} z_1^2 + \frac{1}{2} z_2^2 + \frac{1}{2} z_3^2 + \frac{1}{2} \tilde{w}_g^T \tilde{w}_g + \frac{1}{2} \tilde{w}_h^T \tilde{w}_h \tag{C.5}$$

When $t \to \infty$, then all terms will converge to zero:

$$\begin{aligned} &\tilde{w}_g \to 0 \\ &\tilde{w}_h \to 0 \end{aligned} \tag{C.6}$$

So, (C.4) can be rewritten as follows:

$$\begin{cases} \dot{e}_1 = e_2 \\ \dot{e}_2 = -k_1 e_2 - k_2 e_1 \\ \dot{e}_3 = -k_3 e_3 \end{cases} \tag{C.7}$$

Then we simplify (C.7) to solve as follows:

$$\begin{aligned} &\ddot{e}_1 = \dot{e}_2 = -k_1 e_2 - k_2 e_1 = -k_1 \dot{e}_1 - k_2 e_1 \quad \Rightarrow \\ &\quad \ddot{e}_1 + k_1 \dot{e}_1 + k_2 e_1 = 0 \\ &\ddot{e}_2 = -k_1 \dot{e}_2 - k_2 \dot{e}_1 = -k_1 \dot{e}_2 - k_2 e_2 \quad \Rightarrow \\ &\quad \ddot{e}_2 + k_1 \dot{e}_2 + k_2 e_2 = 0 \\ &\dot{e}_3 = -k_3 e_3 \quad \Rightarrow \quad \dot{e}_3 + k_3 e_3 = 0 \end{aligned} \tag{C.8}$$

$$\begin{cases} \ddot{e}_1 + k_1 \dot{e}_1 + k_2 e_1 = 0 \\ \ddot{e}_2 + k_1 \dot{e}_2 + k_2 e_2 = 0 \\ \dot{e}_3 + k_3 e_3 = 0 \end{cases}$$

Then three differential equations are obtained that they are exponential stable. After solving them, we obtain:

$$\begin{cases} e_1(t) = a_1 e^{\left(\frac{-k_1 + \sqrt{k_1^2 - 4k_2}}{2}\right)t} + a_2 e^{\left(\frac{-k_1 - \sqrt{k_1^2 - 4k_2}}{2}\right)t} \\ e_2(t) = a_3 e^{\left(\frac{-k_1 + \sqrt{k_1^2 - 4k_2}}{2}\right)t} + a_4 e^{\left(\frac{-k_1 - \sqrt{k_1^2 - 4k_2}}{2}\right)t} \\ e_3(t) = a_5 e^{-k_3 t} \end{cases} \tag{C.9}$$

Notice, k_1, k_2, k_3 are positive constant parameters. If $k_1 > 2\sqrt{k_2}$, then $(k_1^2 - 4k_2)$ is positive. When $t \to \infty$, then

$$\begin{cases} \lim\limits_{t \to \infty} e_1(t) \to 0 \\ \lim\limits_{t \to \infty} e_2(t) \to 0 \\ \lim\limits_{t \to \infty} e_3(t) \to 0 \end{cases} \tag{C.10}$$

Therefore, the tracking trajectory is achieved while the dynamics of the gyro are unknown.

References

Chaos, chaos control and chaos synchronization

1. Chen, G.: Controlling Chaos and Bifurcations in Engineering Systems. CRC Press, Boca Raton (1999)
2. Ott, E., Grebogi, C., Yorke, J.A.: Controlling chaos. Phys. Rev. Lett. **64**, 1196–1199 (1990)
3. Chen, G., Dong, X.: From Chaos to Order: Perspectives, Methodologies and Applications. World Scientific, Singapore (1988)
4. Feng, J., Xu, C., Tang, J.: Controlling Chen's chaotic attractor using two different techniques based on parameter identification. J. Chaos Solitons Fractals **32**, 1413–1418 (2007)
5. Harb, A.M., Zahar, A.A., Al Qaisia, A.A., Zohdy, M.A.: Recursive backstepping control of chaotic doffing oscillators. J. Chaos Solitons Fractals **34**, 639–645 (2007)
6. Farivar, F., Shoorehdeli, M.A., Nekoui, M.A., Teshnehlab, M.: Gaussian radial basis adaptive backstepping control for a class of nonlinear systems. J. Appl. Sci. **9**(2), 284–257 (2009)
7. Femat, R., Jauregui-Ortiz, R., Solis-Perales, G.A.: Chaos-based communication scheme via robust asymptotic feedback. IEEE Trans. Circuits Syst. I **48**, 1161–1169 (2001)
8. Pecora, L.M., Carroll, T.L.: Synchronization in chaotic systems. Phys. Rev. Lett. **64**, 821–824 (1990)
9. Yang, J.Z., Hu, G., Xiao, J.H.: Chaos synchronization in coupled chaotic oscillators with multiple positive Lyapunov exponents. Phys. Rev. Lett. **80**, 496 (1998)
10. Shahverdiev, E.M.: Synchronization in systems with multiple time delays. Phys. Rev. E **70**, 067202 (2004)
11. Xu, J.F., Min, L.Q., Chen, G.R.: A chaotic communication scheme based on generalized synchronization and hash functions. Chin. Phys. Lett. **21**, 1445 (2004)

12. Rulkov, N.F., Sushchik, M.M., Tsimring, L.S.: Generalized synchronization of chaos in directionally coupled chaotic systems. Phys. Rev. E **51**, 980 (1995). Abarbanel HDL
13. Rosenblutn, M.G., Pikovsky, A.S., Kurths, J.: Phase synchronization of chaotic oscillators. Phys. Rev. Lett. **76**, 1804 (1996)
14. Cao, L.Y., Lai, Y.C.: Anti-phase synchronism in chaotic systems. Phys. Rev. E **58**, 382–386 (1998)
15. Mainieri, R., Rehacek, J.: Projective synchronization in three-dimensional chaotic systems. Phys. Rev. Lett. **82**, 3042–3045 (1999)
16. Wen, G.L., Xu, D.L.: Nonlinear observer control for full-state projective synchronization in chaotic continuous-time systems. J. Chaos Solitons Fractals **26**, 71 (2005)
17. Wen, G.L., Xu, D.L.: Observer-based control for full-state projective synchronization of a general class of chaotic maps in any dimension. Phys. Lett. A **333**, 420 (2004)
18. Yan, J., Li, C.: Generalized projective synchronization of a unified chaotic system. J. Chaos Solitons Fractals **26**, 1119–1124 (2005)
19. Yan, J.P., Li, C.P.: Generalized projective synchronization for the chaotic Lorenz system and the chaotic Chen system. J. Shanghai Univ. **10**, 299 (2006)
20. Farivar, F., Shoorehdeli, M.A., Nekoui, M.A., Teshnehlab, M.: Generalized projective synchronization for chaotic systems via Gaussian radial basis adaptive backstepping control. J. Chaos Solitons Fractals **42**, 826–839 (2009)
21. Li, G.H.: Modified projective synchronization of chaotic system. J. Chaos Solitons Fractals **32**(5), 1786–1790 (2007)

Chaotic gyroscope system

22. Leipnik, R.B., Newton, T.A.: Double strong attractors in rigid body motion. Phys. Lett. A **86**, 63–67 (1981)
23. Chen, H.K.: Chaos and chaos synchronization of a symmetric gyro with linear-plus-cubic damping. J. Sound Vib. **255**, 719–740 (2002)
24. Ge, Z.-M.: Chaos Control for Rigid Body Systems. Gau Lih Book, Taipei (2002)
25. Chen, H.K.: Chaos and chaos synchronization of a symmetric gyro with linear-pulse-cubic damping. J. Sound Vib. **255**(4), 719–740 (2002)
26. Van Dooren, R.: Comments on chaos and chaos synchronization of a symmetric gyro with linear-plus-cubic damping. J. Sound Vib. **268**, 632–634 (2003)
27. Chen, H.K.: Author's reply. J. Sound Vib. **268**, 635–636 (2003)
28. Chen, H.K., Ge, Z.-M.: Bifurcations and chaos of a two-degree-of-freedom dissipative gyroscope. J. Chaos Solitons Fractals **24**, 125–136 (2005)
29. Chen, H.K., Ge, Z.M.: Bifurcations and chaos of a two-degree-of-freedom dissipative gyroscope. J. Chaos Solitons Fractals **24**, 125–136 (2005)
30. Idowu, B.A., Vincent, U.E., Njah, A.N.: Control and synchronization of chaos in nonlinear gyros via backstepping design. Int. J. Nonlinear Sci. **5**(1), 11–19 (2008)
31. Yan, J.J., Hung, M.L., Lin, J.S., Liao, T.L.: Controlling chaos of a chaotic nonlinear gyro using variable structure control. J. Mech. Syst. Signal Process. **21**, 2515–2522 (2007)
32. Lei, Y., Xu, W., Zheng, H.: Synchronization of two chaotic nonlinear gyros using active control. Phys. Lett. A **343**, 153–158 (2005)
33. Salarieh, H.: Comment on: Synchronization of two chaotic nonlinear gyros using active control [Physics Letter A, Vol. 343, p. 153, 2005]. Phys. Lett. A **372**, 2539–2540 (2008)
34. Idowu, B.A., Vincent, U.E., Njah, A.N.: Generalized adaptive backstepping synchronization for non-identical parametrically excited systems. Nonlinear Anal. Model. Control **14**(2), 165–176 (2009)
35. Yan, J.J., Hung, M.L., Liao, T.L.: Adaptive sliding mode control for synchronization of chaotic gyros with fully unknown parameters. J. Sound Vib. **298**, 298–306 (2006)
36. Yau, H.T.: Nonlinear rule-based controller for chaos synchronization of two gyros with linear-plus-cubic damping. J. Chaos Solitons Fractals **34**, 1357–1365 (2007)
37. Yau, H.T.: Chaos synchronization of two uncertain chaotic nonlinear gyros using fuzzy sliding mode control. J. Mech. Syst. Signal Process. **22**, 408–418 (2008)
38. Farivar, F., Shoorehdeli, M.A., Nekoui, M.A., Teshnehlab, M.: Chaos synchronization of uncertain nonlinear gyros via hybrid control. In: IEEE/ASME International Conference on Advanced Intelligent Mechatronics, pp. 1365–1370 (2009)
39. Farivar, F., Nekoui, M.A., Teshnehlab, M., Shoorehdeli, M.A.: Neural sliding mode control for chaos synchronization of uncertain nonlinear. Adv. Appl. Math. Sci. **4**(1), 41–56 (2010)
40. Salarieh, H., Alasty, A.: Chaos synchronization of nonlinear gyros in presence of stochastic excitation via sliding mode control. J. Sound Vib. **313**, 760–771 (2008)
41. Hung, M.L., Yan, J.J., Liao, T.L.: Generalized projective synchronization of chaotic nonlinear gyros coupled with dead-zone input. J. Chaos Solitons Fractals **35**, 181–187 (2008)
42. Mohseni, S.A., Mohseni, S.M.: Fuzzy neural networks controller for a chaotic nonlinear gyro using sliding mode surfaces. In: International Symposium on Industrial Electronics (ISIE), Cambridge, pp. 1150–1153 (2008)
43. Ge, Z.M., Lee, J.K.: Chaos synchronization and parameter identification for gyroscope system. Appl. Math. Comput. **163**, 667–682 (2005)
44. Yau, H.T.: Generalized projective chaos synchronization of gyroscope systems subjected to dead-zone nonlinear inputs. Phys. Lett. A **372**, 2380–2385 (2008)
45. Yau, H.T.: Synchronization and anti-synchronization coexist in two-degree-of-freedom dissipative gyroscope with nonlinear inputs. Nonlinear Anal., Real World Appl. **9**, 2253–2261 (2008)

Backstepping control and neural backstepping control

46. Yassen, M.T.: Chaos control of chaotic dynamical systems using backstepping design. J. Chaos Solitons Fractals **27**, 537–548 (2006)
47. Khalil, H.: Nonlinear Sytems, 3rd edn. Prentice-Hall, New York (2002)
48. Peng, Y.F., Lin, M.H., Chiu, C.H., Lin, C.M.: Development of adaptive intelligent backstepping tracking control for uncertain chaotic systems. In: 6th International Conference on Machine Learning and Cybernetics, pp. 2037–2043 (2007)

49. Kwan, C., Lewis, F.L.: Robust backstepping control of nonlinear systems using neural networks. IEEE Trans. Syst. Man Cybern. A **30**(5), 753–766 (2000)
50. Lewis, F.L., Yesildirek, A., Liu, K.: Robust backstepping control of induction motor using neural networks. IEEE Trans. Neural Netw. **11**(6), 1178–1187 (2000)
51. Zhang, Y., Peng, P.Y., Jiang, Z.P.: Stable neural controller design for unknown nonlinear systems using backstepping. IEEE Trans. Neural Netw. **11**(5), 1347–1359 (2000)
52. Chen, B., Liu, X., Tong, S.: Adaptive fuzzy output tracking control of MIMO nonlinear uncertain systems. IEEE Trans. Fuzzy Syst. **15**(2), 287–300 (2007)
53. Hsu, C.F., Lin, C.M., Lee, T.T.: Wavelet adaptive backstepping control for a class of nonlinear systems. IEEE Trans. Neural Netw. **17**(5), 1175–1183 (2006)
54. He, P., Jagannathan, S.: Neuroemission controller for reducing cyclic dispersion in lean combustion spark ignition engines. J. Autom. **41**, 1133–1142 (2005)
55. Jagannathan, S.: Discrete-time adaptive control of feedback linearizable nonlinear systems. Proc. IEEE Conf. Decis. Control **3**, 1704–1709 (1996)
56. Jagannathan, S., Lewis, F.L.: Discrete-time neural net controller for a class of nonlinear dynamical systems. IEEE Trans. Autom. Control **41**(11), 1693–1699 (1996)
57. Jagannathan, S., Lewis, F.L.: Multilayer discrete-time neural-net controller with guaranteed performance. IEEE Trans. Neural Netw. **7**(1), 107–130 (1996)
58. Jagannathan, S., Commuri, S., Lewis, F.L.: Robust backstepping control of robotic systems using neural networks. J. Intell. Robot. Syst. **23**, 105–128 (1998)
59. Jagannathan, S.: Control of a class of nonlinear discrete-time systems using multilayer neural networks. IEEE Trans. Neural Netw. **12**(5), 1113–1120 (2001)
60. Lewis, F.L., Jagannathan, S., Yesildirek, A.: Neural Network Control of Robot Manipulators and Nonlinear Systems. Taylor & Francis, London (1999)
61. Alanis, A.Y., Sanchez, E.N., Loukianov, A.G.: Discrete-time adaptive backstepping nonlinear control via high-order neural networks. IEEE Trans. Neural Netw. **18**(4), 1185–1195 (2007)
62. Polycarpou, M.M.: Stable adaptive neural control scheme for nonlinear systems. IEEE Trans. Autom. Control **41**(3), 447–451 (1996)
63. Lin, F.J., Wai, R.J., Chen, H.P.: A PM synchronous servo motor drive with an on-line trained fuzzy neural network controller. IEEE Trans. Energy Convers. **13**(4), 319–325 (1998)
64. Wang, H., Wang, Y.: Neural-network-based fault-tolerant control of unknown nonlinear systems. Proc. IEE Conf. Control Theory Appl. **146**, 389–398 (1999)
65. Lin, C.M., Hsu, C.F.: Neural-network-based adaptive control for induction servomotor drive system. IEEE Trans. Ind. Electron. **49**(1), 115–123 (2002)
66. Lin, C.M., Hsu, C.F.: Neural network hybrid control for antilock braking systems. IEEE Trans. Neural Netw. **14**(2), 351–359 (2003)
67. Wang, D., Huang, J.: Neural network-based adaptive dynamic surface control for a class of uncertain nonlinear systems in strict-feedback from. IEEE Trans. Neural Netw. **16**(1), 195–202 (2005)